# Week 4

GEO 225 Lecture #1 Heat Flow

Reading Ch. 8 Judson & Richardson

Straw poll:

(1) How many people think it gets cooler as you go down into the ⊕? How many think it gets hotter?

(2) How many think the interior of the ⊕ is molten? Volcanoes?

(3) Below where do you think it's molten?

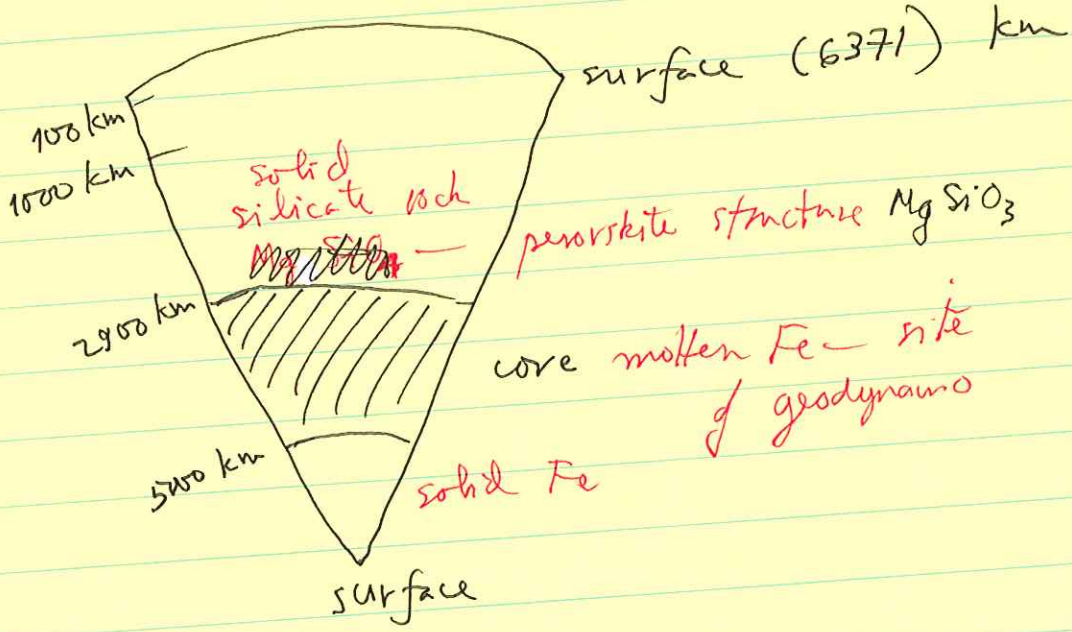


Start with some elementary facts regarding units.

Celsius Fahrenheit

Temperature:

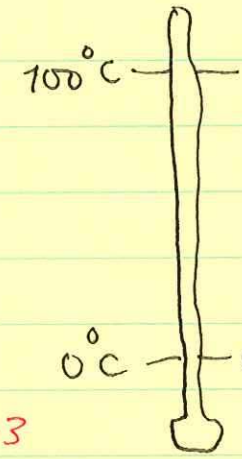


water boils at sea level

water freezes at sea level

Kelvins

also: $T(K) = T(°C) + 273$

temperature above absolute zero

$$T(°F) = \frac{9}{5} T(°C) + 32$$

We will always use °C. (or K)

Heat is a form of energy — measured in Joules

$$1 \text{ Joule} = 1 \frac{kg\ m^2}{s^2} \qquad (E = mc^2)$$

Power is a measure of the rate at which energy is produced, or consumed, or used, or expended

$$1 \text{ watt} = 1 \frac{J}{s}$$

A 60-watt light bulb consumes 60 Joules of energy every second that it is turned on.

There are also antiquated units for energy, which date to the time when heat was thought to be a separate substance — phlogiston

1 calorie is by definition the amount of heat required to raise the temperature of one gm of $H_2O$ by 1°C.

| 1 cal = 4.184 J |
|---|

The energy content of food is measured in Calories
↑
cap. C

1 Calorie = 1 kcal = 1000 cal
= 4184 J

There are three modes of heat transfer:

↓ we will study this in 4th quarter of course

1. radiation — this is how we get heat from the sun — in the form of photons — not significant within the ⊕ (or any opaque solid material)

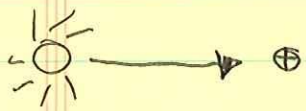

2. conduction — this is how a skillet on a stove gets hot

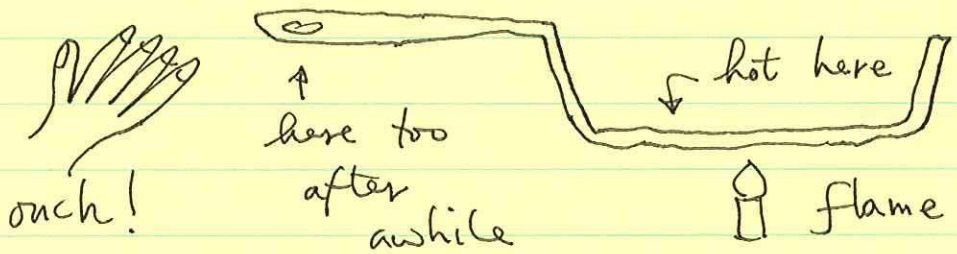


3. convection — put a pot of $H_2O$ on stove

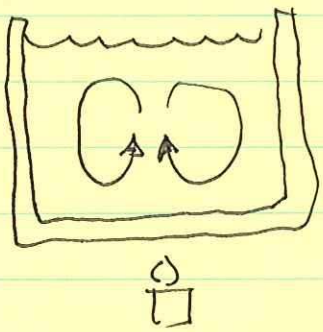

before it boils — by conduction

after it boils — heat is convected to top — physical exchange of hot & cold water.

Both conduction & convection are important in the Earth — conduction dominates in the uppermost ~ 100 km (except in geothermal areas such as Yellowstone and Iceland)

Heat conduction — consider the amount of heat flowing through an area in a given time

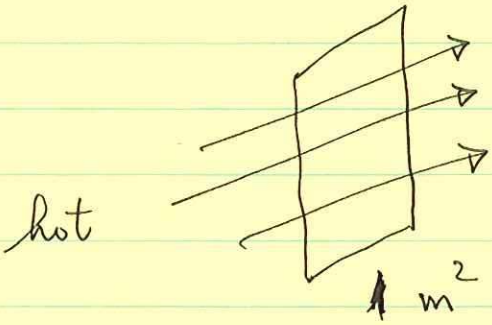


units of heat flow

$J/m^2\text{-}s = W/m^2$

Heat flow within the ⊕ is small (usually expressed as $mW/m^2$).

Consider the skillet again

$T$ temp $T_1$ ——— $z_1$ $z$

$T+dT$ temp $T_2$ ——— $z_2$ $z+dz$

$T_2 > T_1$

$$q = \kappa \frac{T+dT-T}{z+dz-z} = \kappa \frac{dT}{dz}$$

heat flow $q = \kappa \dfrac{T_2 - T_1}{z_2 - z_1}$ or

$$q = \kappa \frac{dT}{dz}$$

$\kappa$ = kappa

$\kappa$ ↗ thermal conductivity

$\frac{dT}{dz}$ ↑ temperature gradient °C/m

The thermal conductivity $\kappa$ is a material property

units : $\frac{W/m^2}{{}^\circ C/m} = \frac{W}{m\,{}^\circ C}$

| material | $\kappa$ ( $W/(m\,{}^\circ C)$ ) | |
|---|---|---|
| Cu | 400 | good skillets |
| Al | 240 | forget this one |
| Fe | 80 | |
| dry upper mantle rocks (high T olivine) | 3 — typical of hard dry rocks | |
| water | 0.6 | |
| soil | about the same | |
| styrofoam | 0.03 — | good insulation |

factor of $10^5$ variation

conductors vs. insulators

Heat flow from the surface of the ⊕ is most easily measured in the oceans. Probe 3–10 m in length

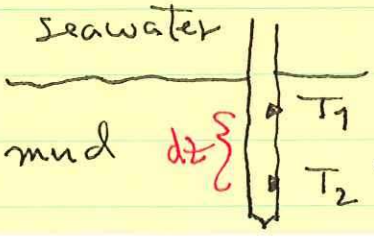

$$q = \kappa \frac{dT}{dz}$$

Typically $\kappa_{mud} \sim 0.5 \frac{W}{m\,^\circ C}$

$dT/dz \sim 0.1\ ^\circ/m$ — easily measured — very stable thermal environment: no diurnal fluctuations as on land or annual

on land need much deeper holes to get below seasonal cycle

Mean surface heat flow

$$\bar{q} = 60 \frac{mW}{m^2}$$

— heat flow through $1000\ m^2$ = $\frac{1}{3}$ football field

= 30m x 30m would heat me 60W bulb

In comparison: $5 \cdot 10^{14}\ m^2$

$\bar{q}$ x surface area of $\oplus$ $(4\pi a^2)$

$= 3 \cdot 10^{13}$ W conductive heat flow

enough to light $5 \cdot 10^{11}$ 60-watt light bulbs

The solar constant is 1370 W/m²

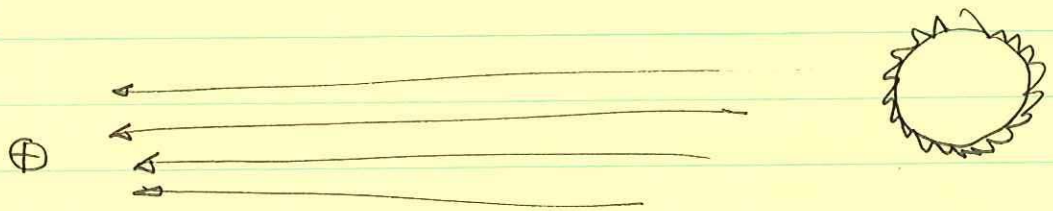

Averaged over ⊕ surface: $\frac{1370}{4} = 340\ W/m^2$

Total solar energy striking the ⊕

$1.7 \cdot 10^{17}\ W$

another comparison — total world fossil fuel consumption $\sim 10^{13}\ W$

of this ~70% absorbed by atmosphere and surface, ~30% reflected back into space

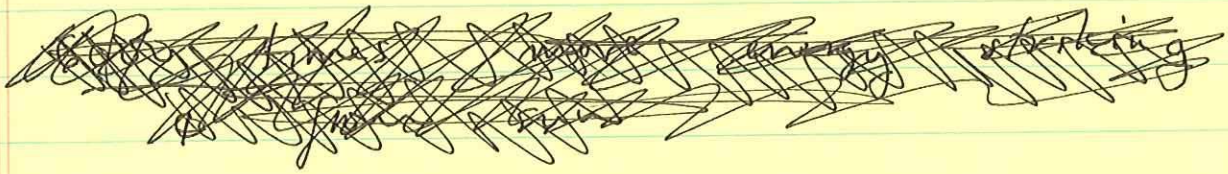

4000 times more energy absorbed from sun than escaping from interior.

fossil fuel consumption ~ 1/3 x total terrestrial heat flow

The thermal conductivity of typical crustal rock (not porous mud) is $\kappa_{rock} = 3\ W/m^\circ C$.

so that $3.20 \cdot 10^{-3} = 60 \frac{mW}{m^2}$

Typical geotherm ~~25~~ 20°C / km

I gets hotter by this amount every km we drill down (on land or in basalt beneath seafloor seds)

How hot would it be at center of ⊕ if this gradient were maintained all the way down?

20
~~25~~ °C/km × 6371 km
130,000 °C
= ~~160,000 °C~~ !

in fact this was widely believed until late 19th century (Kelvin & Darwin — fortnightly tides)

Almost entire interior of ⊕ would be molten if this were true

solidus — T (°C) at which the lowest-melting component of a multi-component system melts.

liquidus — T (°C) at which all components have melted

Discuss ellipsoidal shape of ⊕: Newton

Seismic evidence for solidity of mantle → temperature gradient must decrease with depth

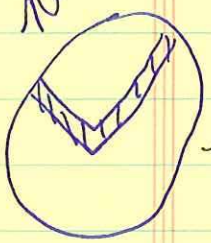

Roughly speaking, the temperature increases by ~ 20 ~~25~~ °C/km down to about [redacted] 50 km depth.

The uppermost ~100 km of the ⊕ surface is the region where the heat transport from the interior is dominated by conduction

lithosphere : mechanically strong; cannot flow in response to stresses; heat transport dominated by conduction

asthenosphere (and underlying mantle) in a state of active convection. this is the dominant mode of heat transfer

$$\frac{dT}{dz} \sim 0.6\ ^\circ\text{C/km}$$

adiabatic gradient

then: 1350° + (0.6)(2800 km) ≈ 3000°C at CMB.

10 – 100 times less than conductive gradient

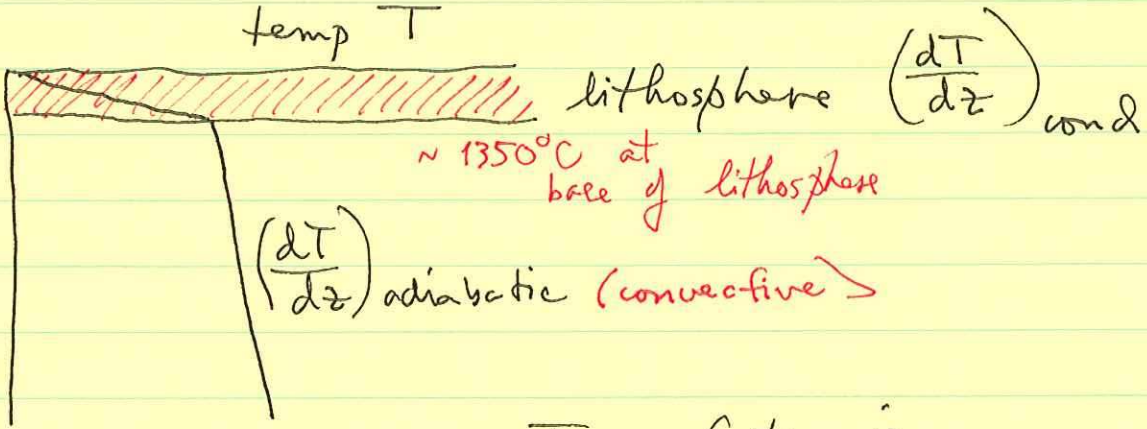


note – the (subsolidus) convective velocities are very slow (cm/yr)

In fact is rounded off as shown in J & R Figure 8.12

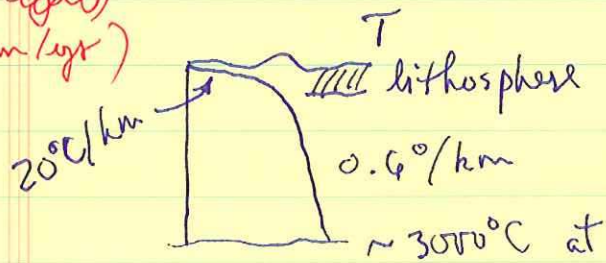

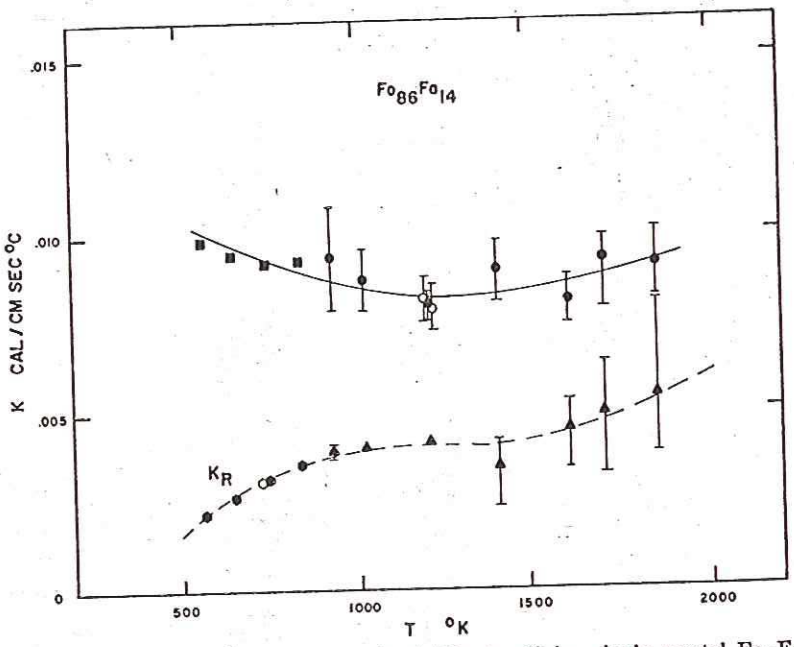


Fig. 5b. Total and radiative thermal conductivities in olivine single crystal $Fo_{86}Fa_{14}$. Open circles are points measured at descending temperature. Solution below 900°K are obtained by using assumed values of $\kappa_L$.

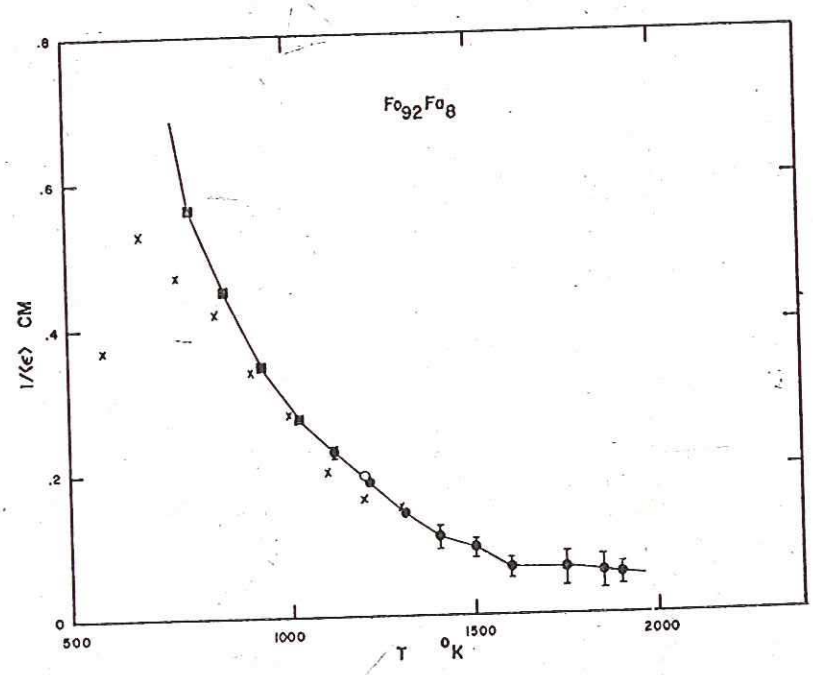


Fig. 6a. Photon mean free path in olivine single crystal $Fo_{92}Fa_8$. The open circle is a point measured at descending temperature. Solutions below 1100°K are obtained by using assumed values of $\kappa_L$. The crosses are data of *Fukao et al.* [1968] for a crystal of olivine composition $Fo_{88}Fa_{12}$.

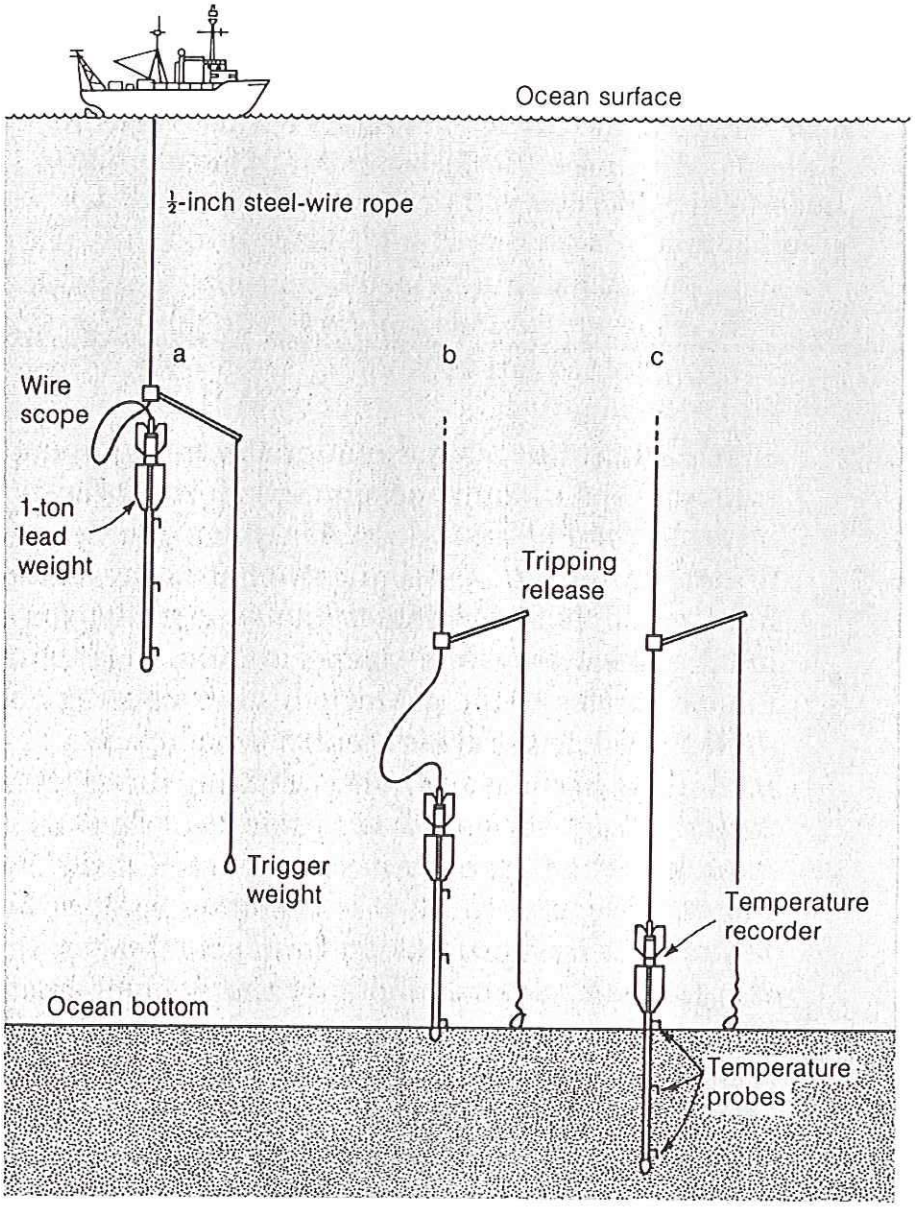


**igure 13-6**
Heat flowing out of the sea is measured by plunging . core tube about 10 meters long into the sediments. Thermometers on the side of the tube record the emperature increase with depth, and the thermal onductivity of the sediments is measured when the ore is retrieved. The product gives the heat flow.

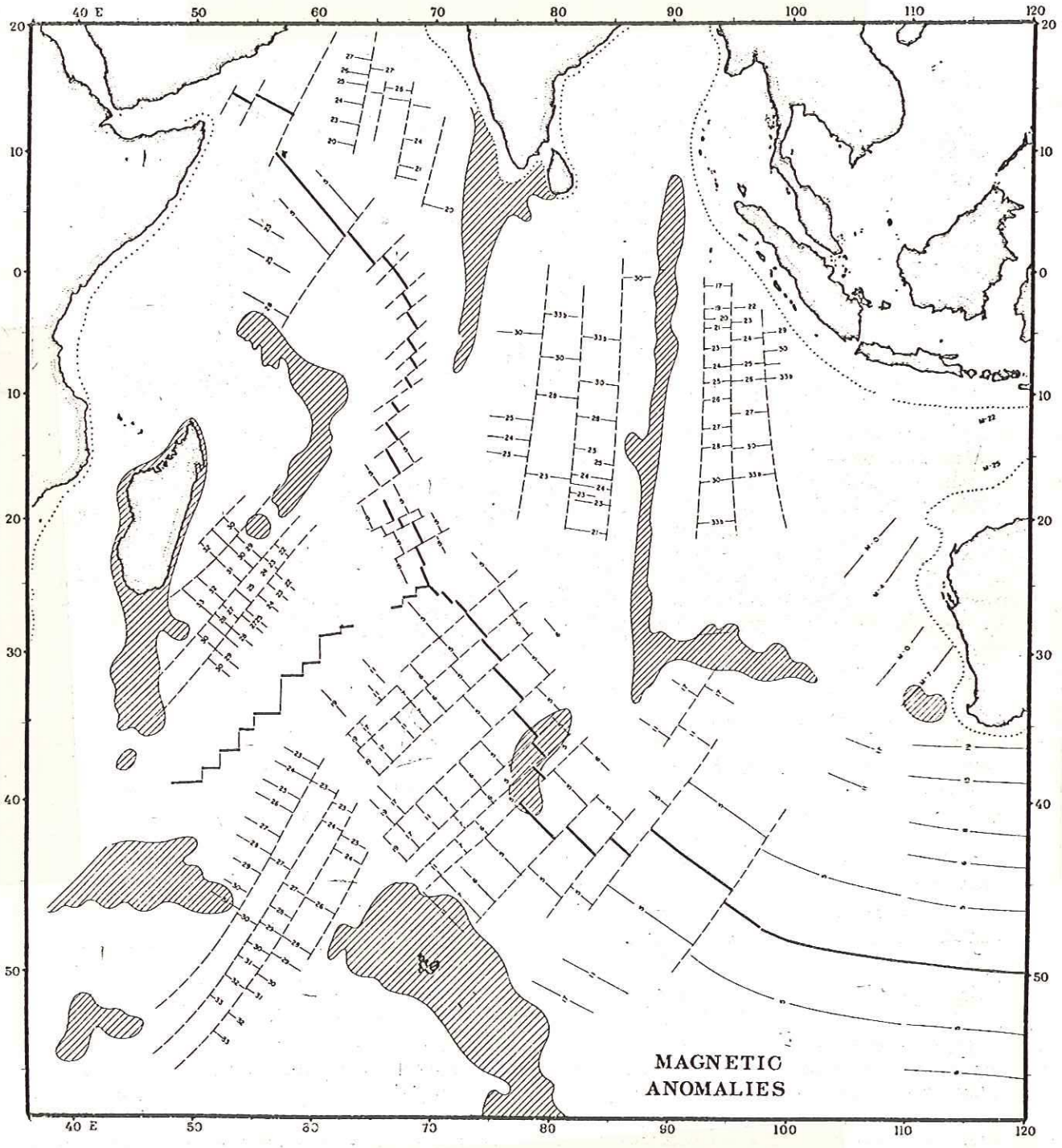


Fig. 6. Identifiable magnetic anomalies in Indian Ocean. For sources, see text. Hachures represent shoal regions of Figure 1.

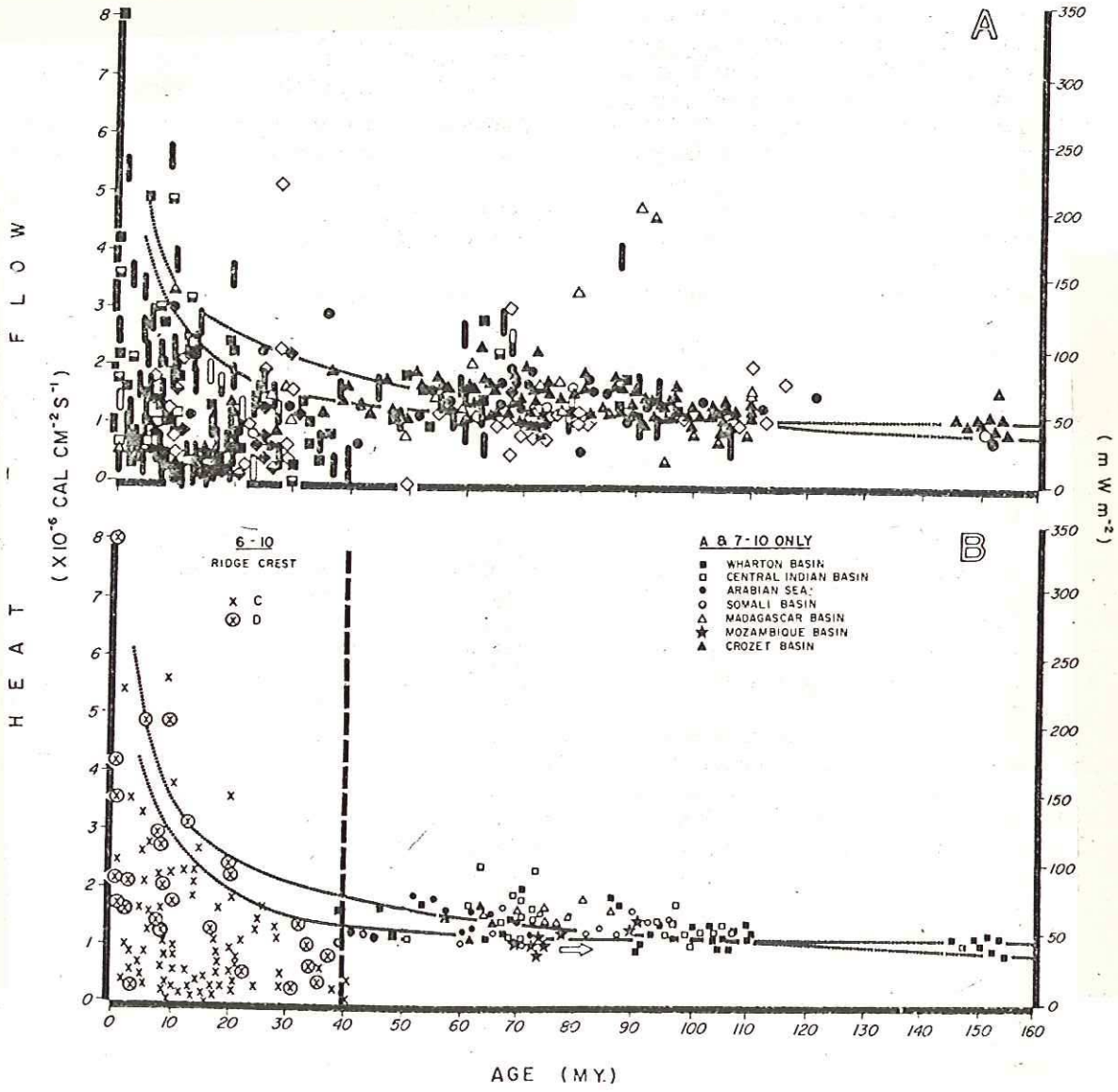


Fig. 9. Heat flow versus age in the Indian Ocean. (*a*) All the data. (*b*) Filtered data. Notice that the filtering removes much scatter but does not change the mean of values older than 50 m.y. B.P. The arrow refers to the Mozambique Basin values that appear to be from older sea floor than that indicated by DSDP hole ages in the basin. Solid curves are from *Sclater and Francheteau* [1970] and *Parker and Oldenburg* [1973].

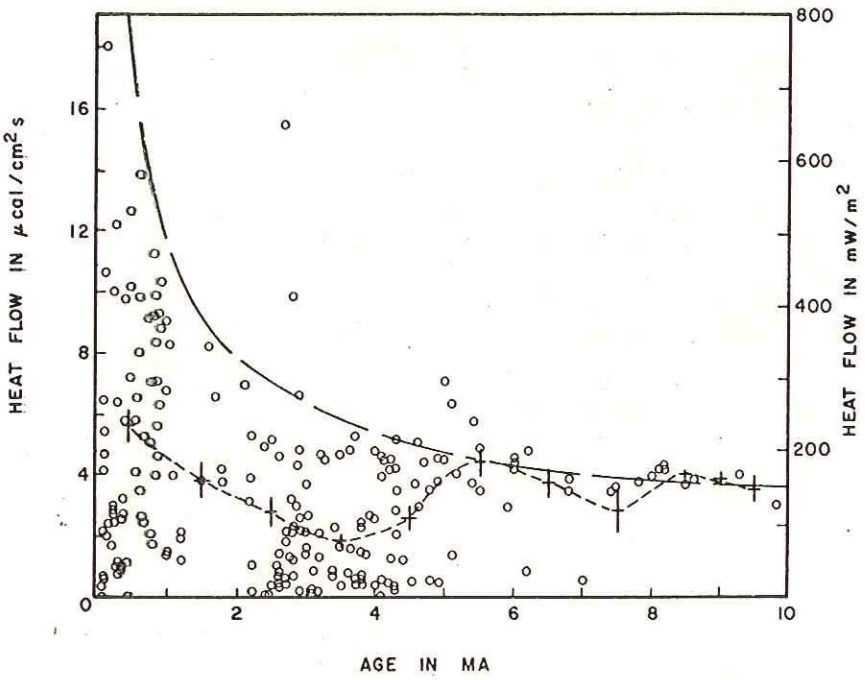


Fig. 5. Heat flow values plotted as a function of age on the Galapagos spreading center. Only those values which are on oceanic crust of well-defined age were used for this plot. Circles represent heat flow values. Pluses are 1-m.y. means. The long-dashed curve is the heat flow expected from the thermal model of *Parsons and Sclater* [1977], and the short-dashed curve connects the mean of the observed data [after *Anderson and Hobart*, 1976].

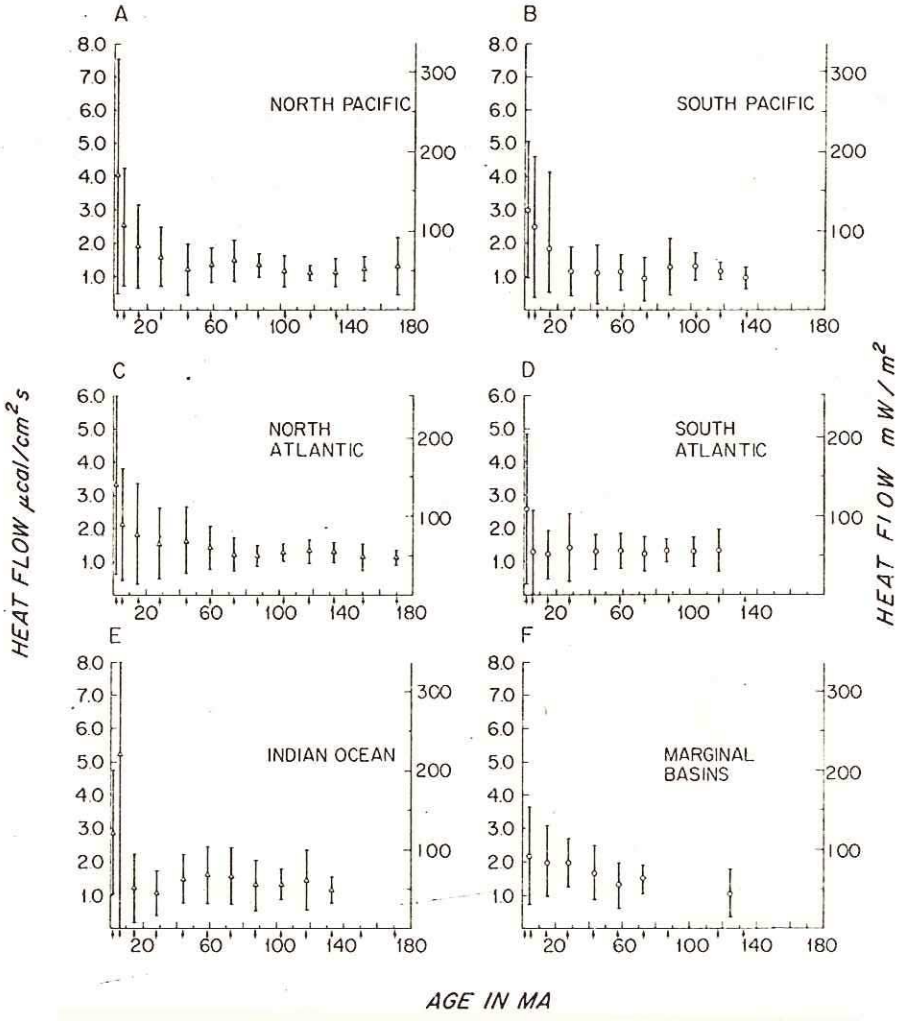


Fig. 1. Mean heat flow and standard deviation as a function of age for five major oceans and the marginal basins.

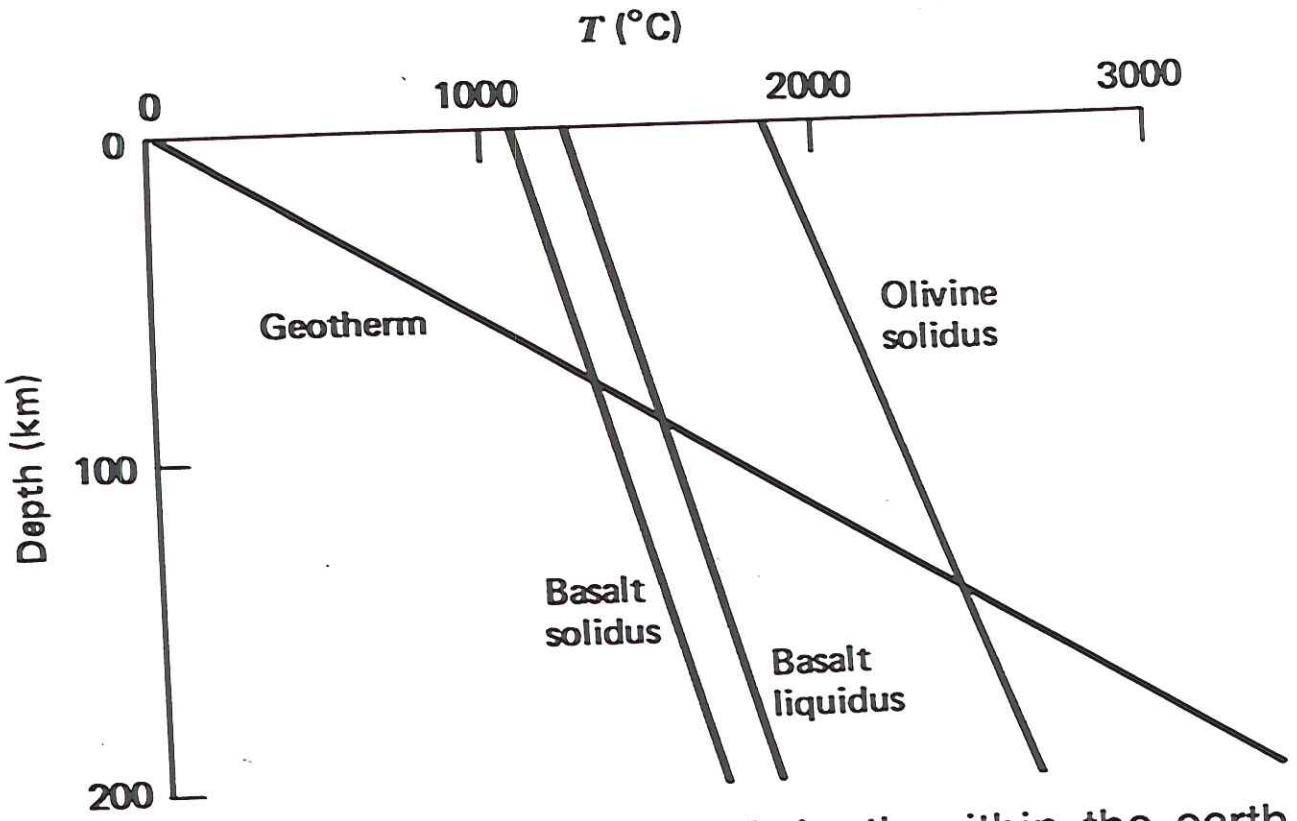


**Figure 4-8** Temperature as a function of depth within the earth assuming heat transport is by conduction (conduction geotherm). Also included are the solidus and liquidus of basalt and the solidus of peridotite.

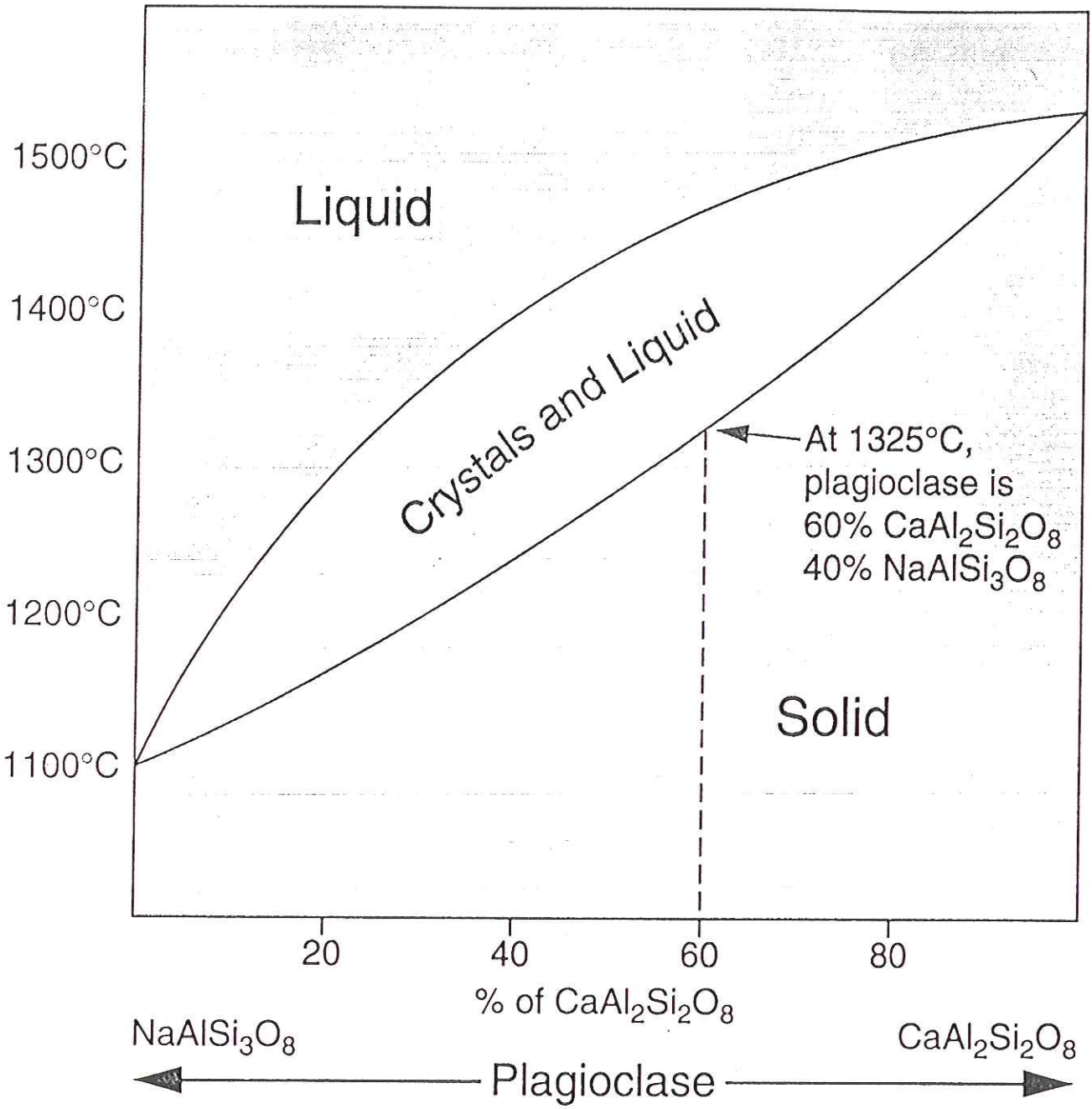


**FIGURE 2.27** This diagram shows how the composition of plagioclase changes with temperature, which increases upwards. The composition of a crystal forming at any temperature of interest can be read by looking at the lower line, which separates the region marked "solid" from the one marked "crystals and liquid." For example, at about 1325°C a newly crystallized plagioclase has a composition 60% of the way between $NaAlSi_3O_8$ and $CaAl_2Si_2O_8$, or $Na_{0.4}Ca_{0.6}Al_{1.6}Si_{2.4}O_8$.

**FIGURE 8.12** Estimated average geotherms in continental and oceanic lithosphere. The convecting mantle is nearer to the surface in the ocean basins than under the continents, so high temperatures are reached at relatively shallow depths.

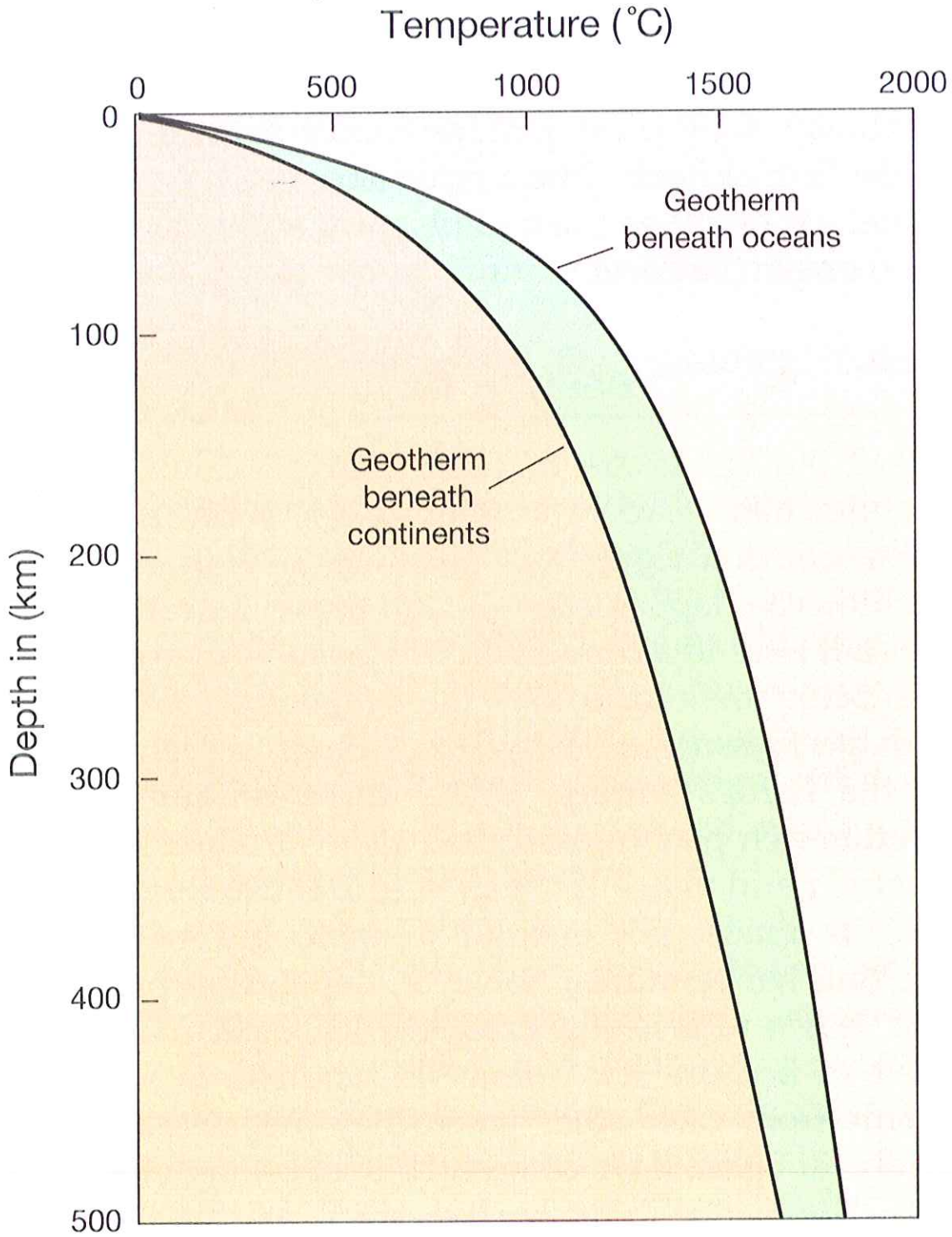

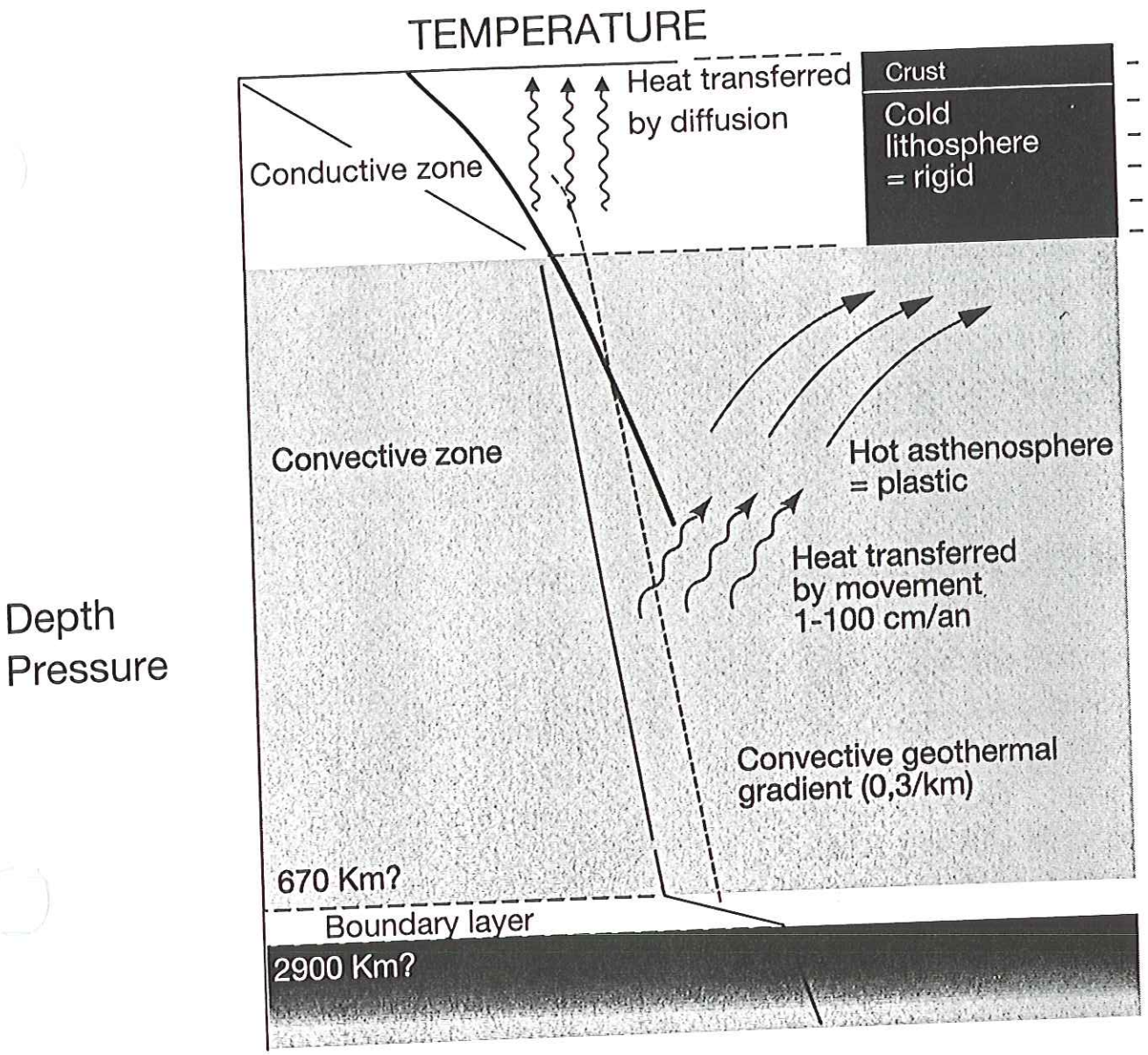


**Figure 2.7**
Simplified diagram of temperature vs. depth (cf. Fig. 2.6) illustrating the relationship between heat transfer and mechanical structure within the mantle. The heat is transferred by diffusion (conduction) in the rigid lithosphere and the boundary layers at depth and by movement of material (convection) in the convection cells. The different slopes of the geotherms (cf. Fig. 2.6) correspond to the different types of transfer. The *thicker line* (solidus) corresponds to the onset of melting in the mantle (cf. Chap. 6). The *dashed line* illustrates the path of a plume rising from a deep boundary layer. It intersects the solidus at great depth, which may explain the abundance of melting (Chap. 6)

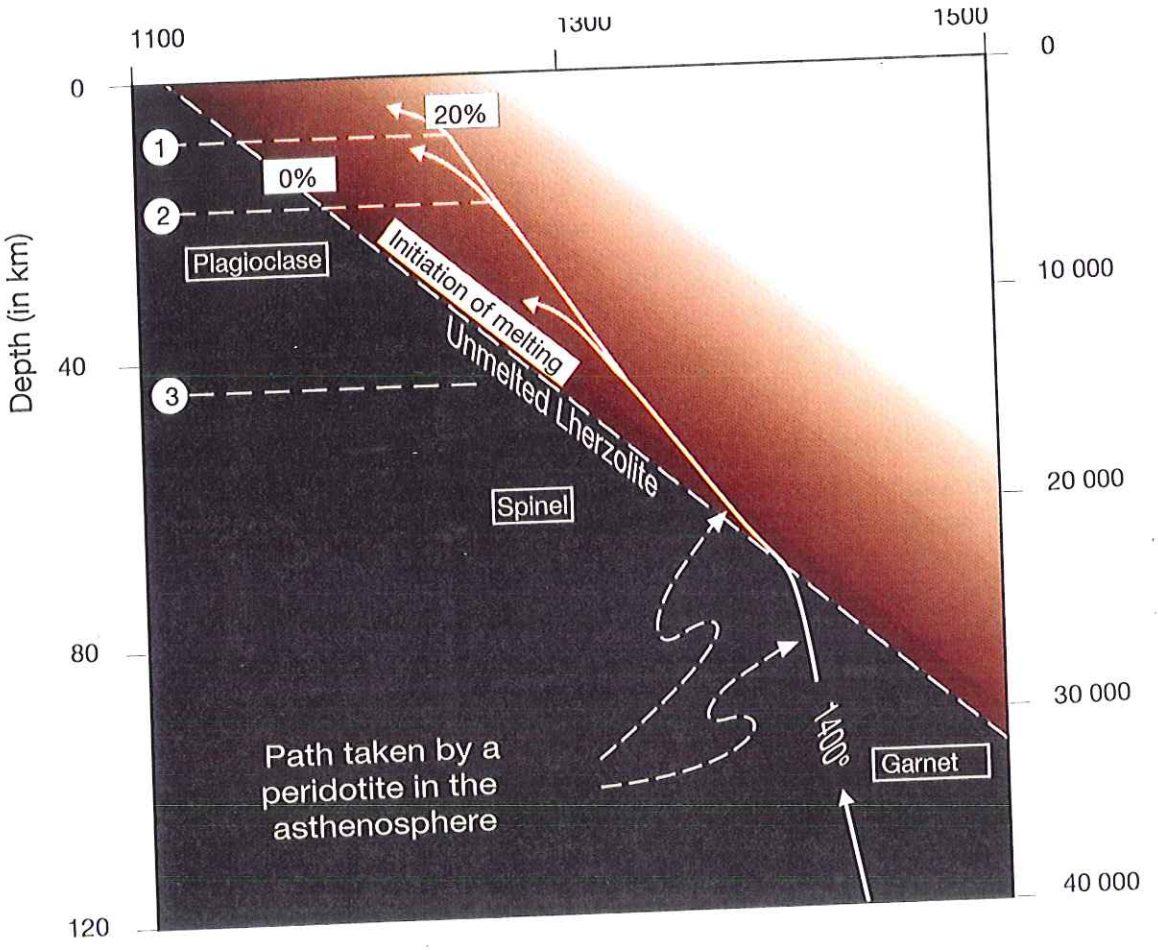


**Figure 6.6**
Diagram of the evolution of temperature and melting of a mantle peridotite during ascent to the surface. The trajectory follows the *white arrows from bottom to top.* Rising within the dry asthenosphere (*dark red*), the peridotite starts to melt when it crosses into the lighter-coloured areas. The increasing degree of melting is indicated by *increasingly lighter red colour.* The diagram contains two other pieces of information: In the "solid" domain (*dark red*), depending on the depth, the peridotite may contain garnet (below 75 km), spinel (30–75 km), or plagioclase (above 30 km). *1*, *2*, and *3* correspond respectively to three possible trajectories, depending on the depth at which the rising peridotite becomes incorporated in the lithosphere (cf. Chap. 8)

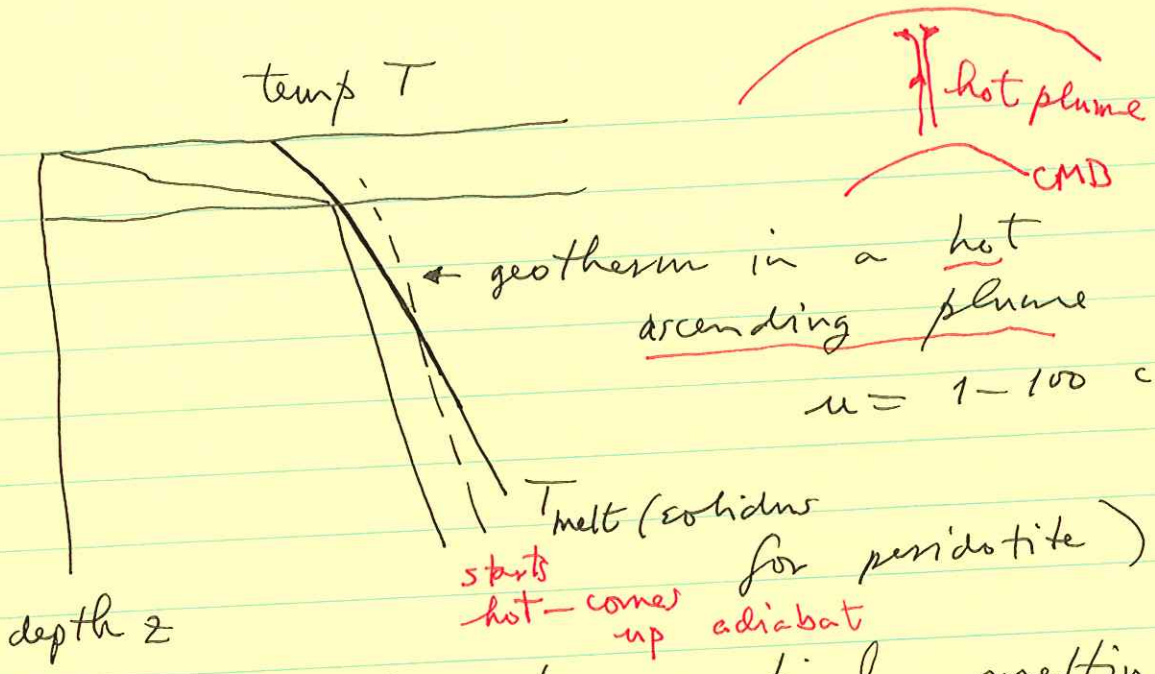


leads to partial melting above ascending plumes

Also beneath mid-ocean ridges where mantle peridotite wells up to replace that removed by spreading.

The resulting axial volcanism is responsible for the 6 km thick basaltic oceanic crust.

The underlying mantle material is the depleted refractory residual.

Cross-sections of oceanic crust are exposed in a few places on ⊕. They are called ophiolites

# Mechanism for melting beneath mid-ocean ridges

On flank of ridge

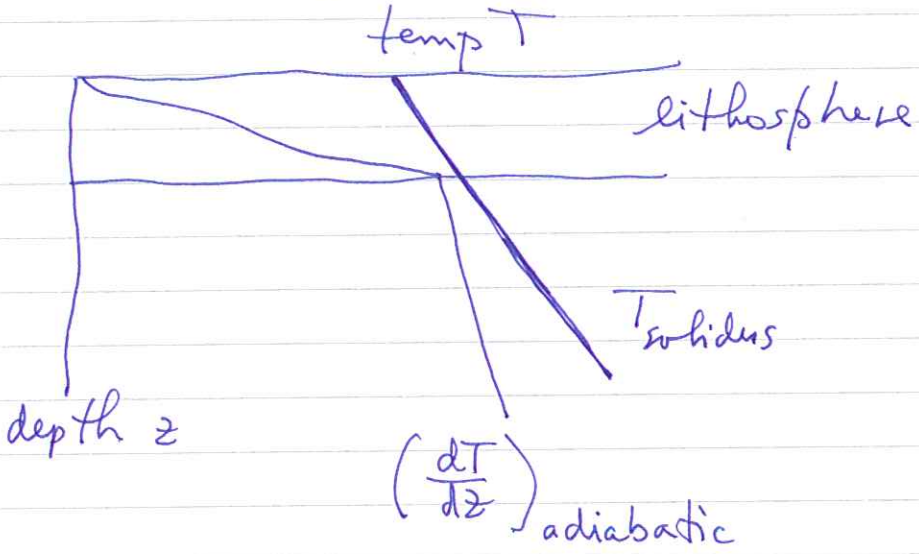


But at ridge, lithosphere is rifted

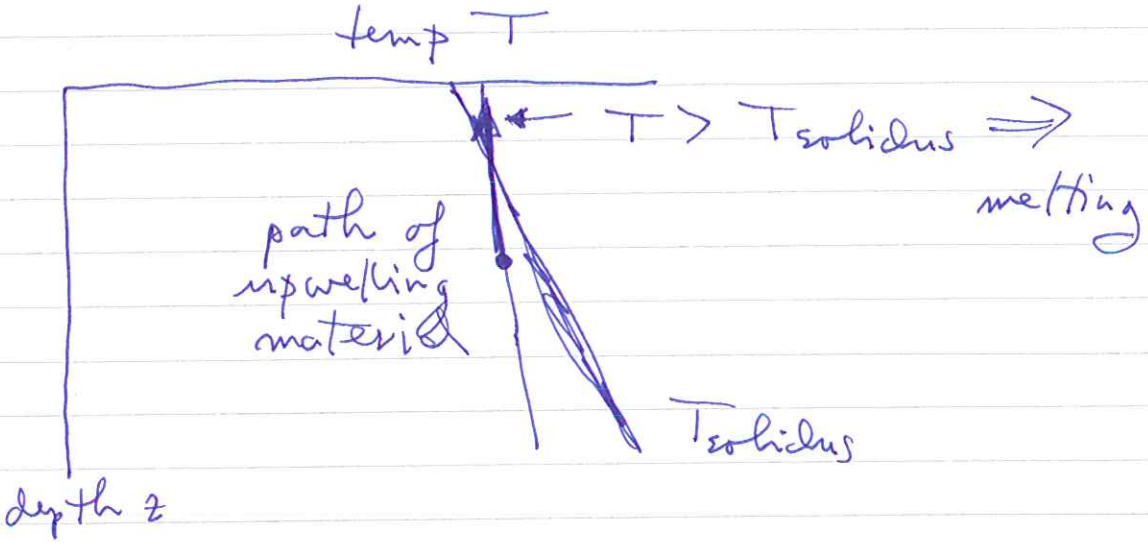

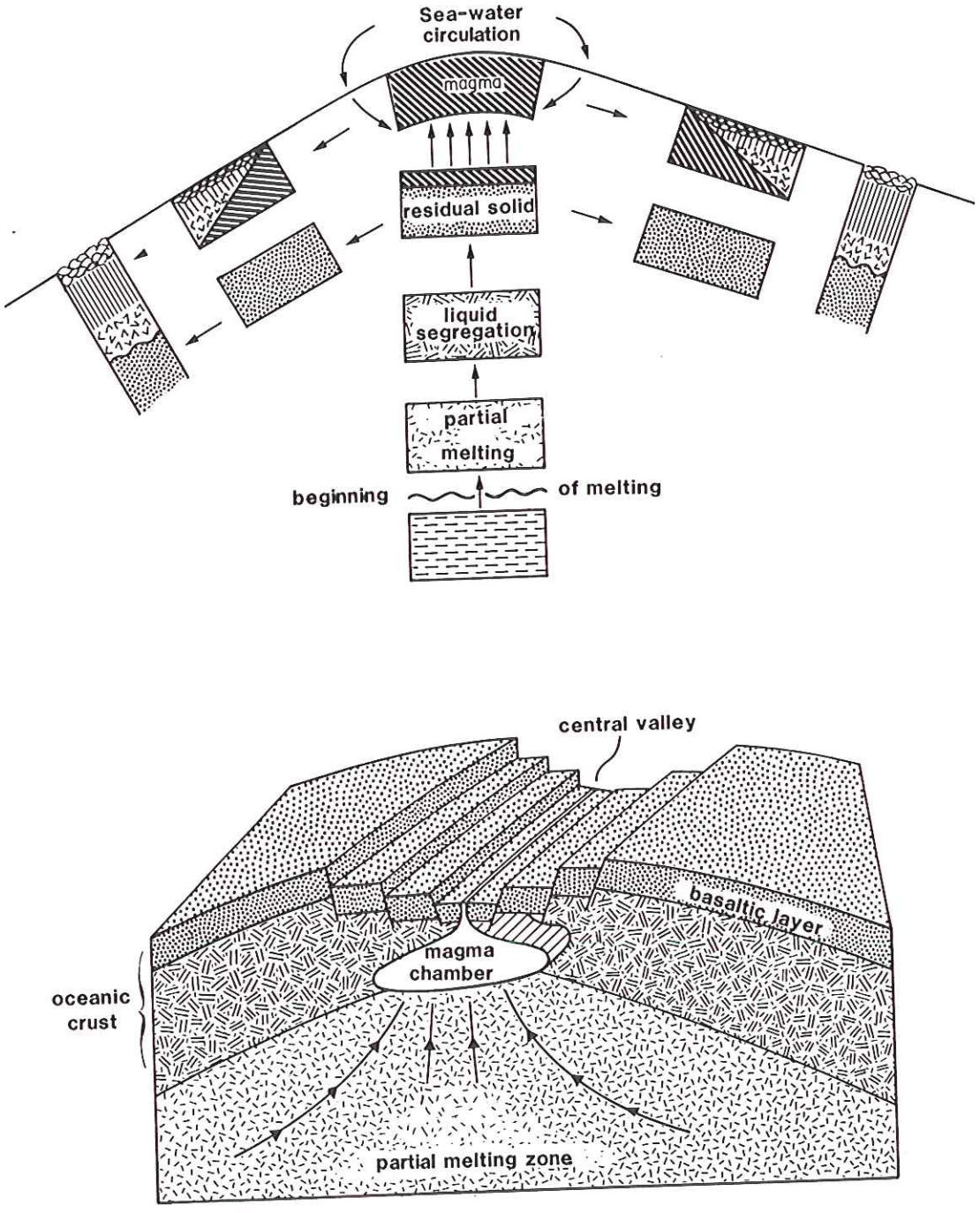


FIGURE 55 The creation of oceanic lithosphere. Material from the mantle rises beneath a ridge axis. During its ascent melting occurs and the liquid thus formed rises faster than surrounding unmelted material. Near the surface the liquid (which forms the crust) cools and interacts with seawater. Then the liquid and residual material spread horizontally away from the spreading axis. On the bottom is a block diagram of a slow-spreading ridge (spreading at, say, a rate on the order of 2 centimeters per year) that shows how the processes of lithosphere creation may occur in a more realistic scenario.

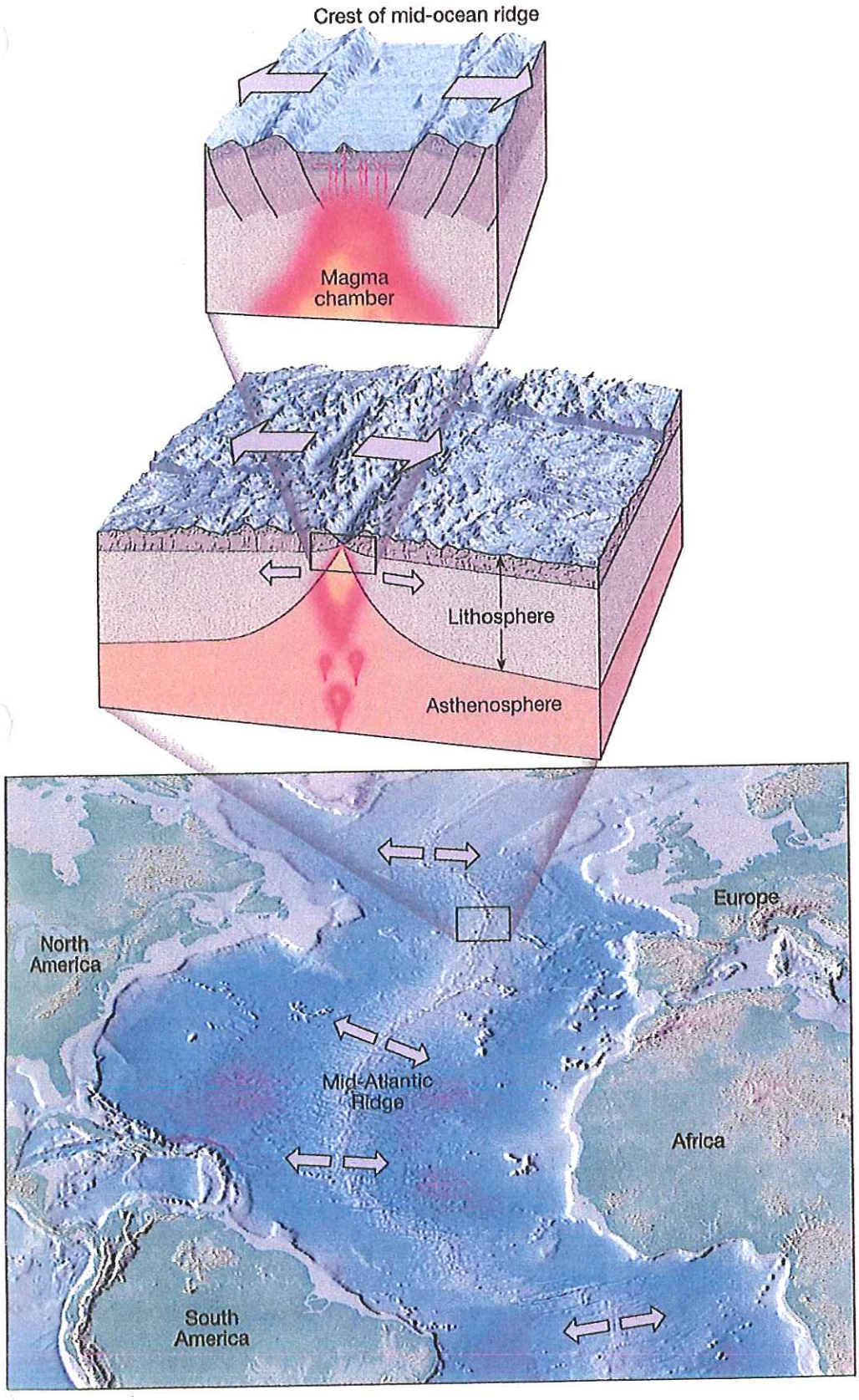


**Figure 19.19** Most divergent plate boundaries are situated along the crests of oceanic ridges.

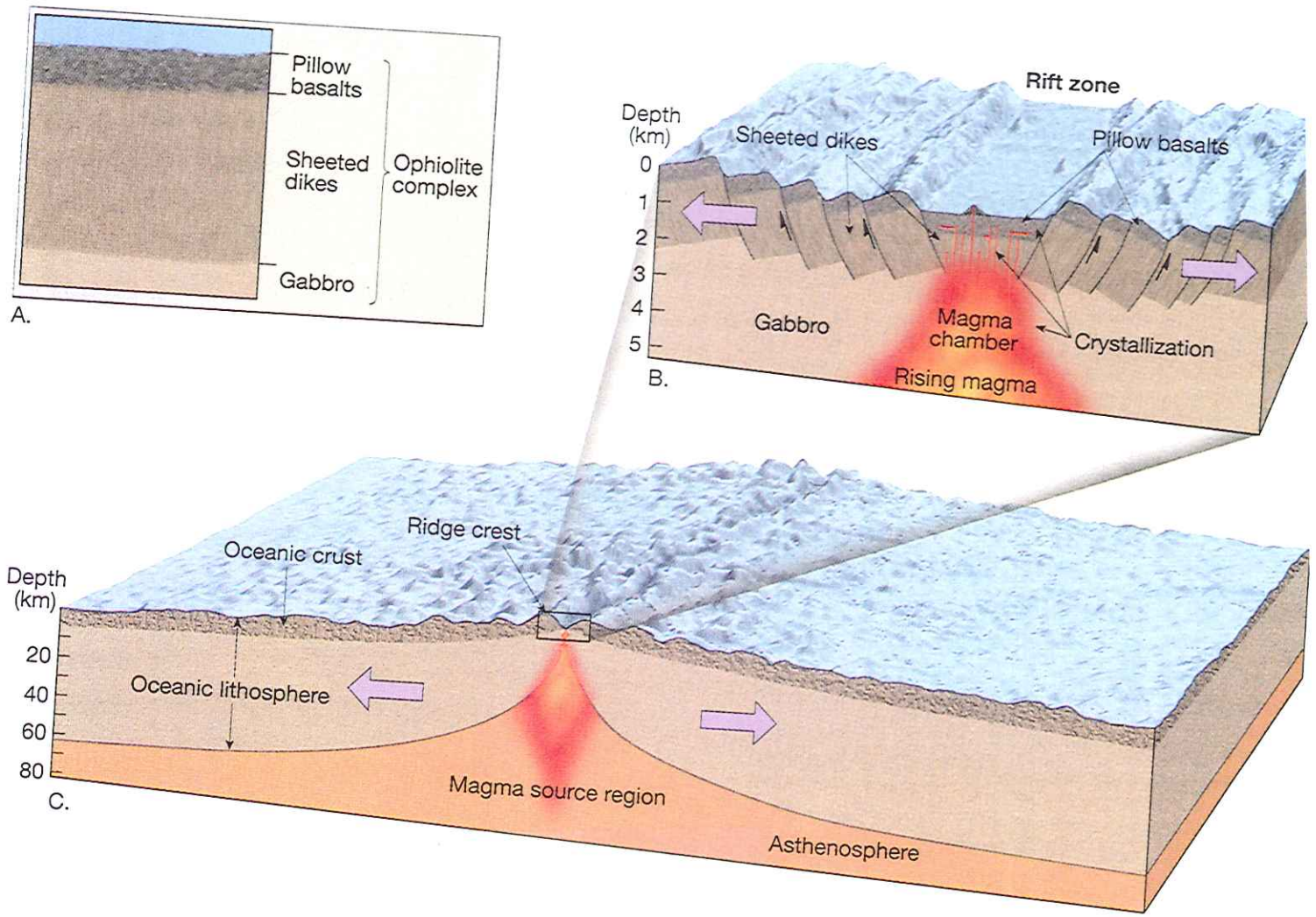
Pillow basalts
Sheeted dikes
Ophiolite complex
Gabbro
A.
Rift zone
Depth (km)
0
1
2
3
4
5
Sheeted dikes
Pillow basalts
Gabbro
Magma chamber
Crystallization
Rising magma
B.
Ridge crest
Oceanic crust
Depth (km)
20
40
60
80
Oceanic lithosphere
Magma source region
Asthenosphere
C.

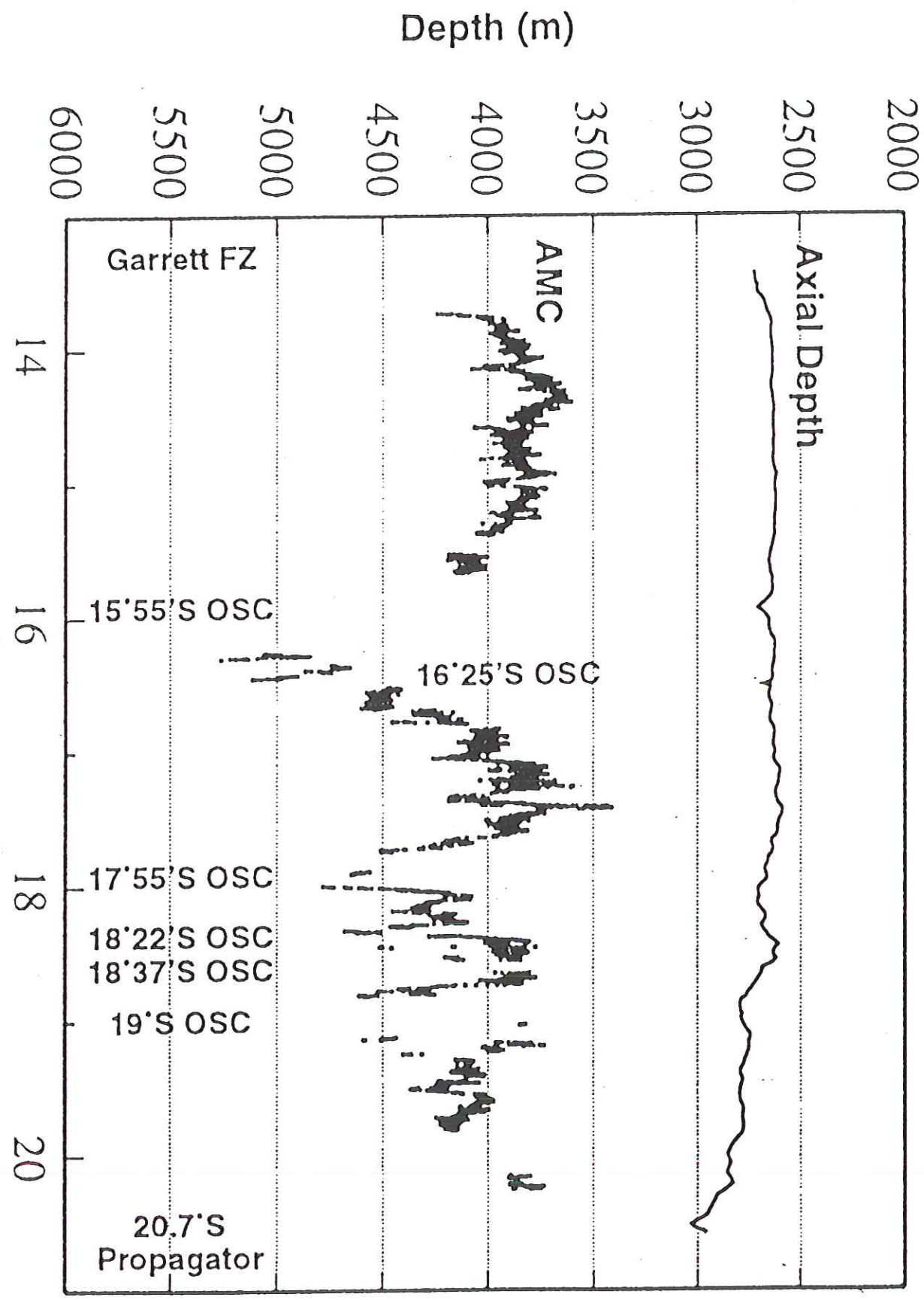
Depth (m)
6000
5500
5000
4500
4000
3500
3000
2500
2000
Axial Depth
AMC
Garrett FZ
14
16
18
20
15°55'S OSC
16°25'S OSC
17°55'S OSC
18°22'S OSC
18°37'S OSC
19°S OSC
20.7°S
Propagator

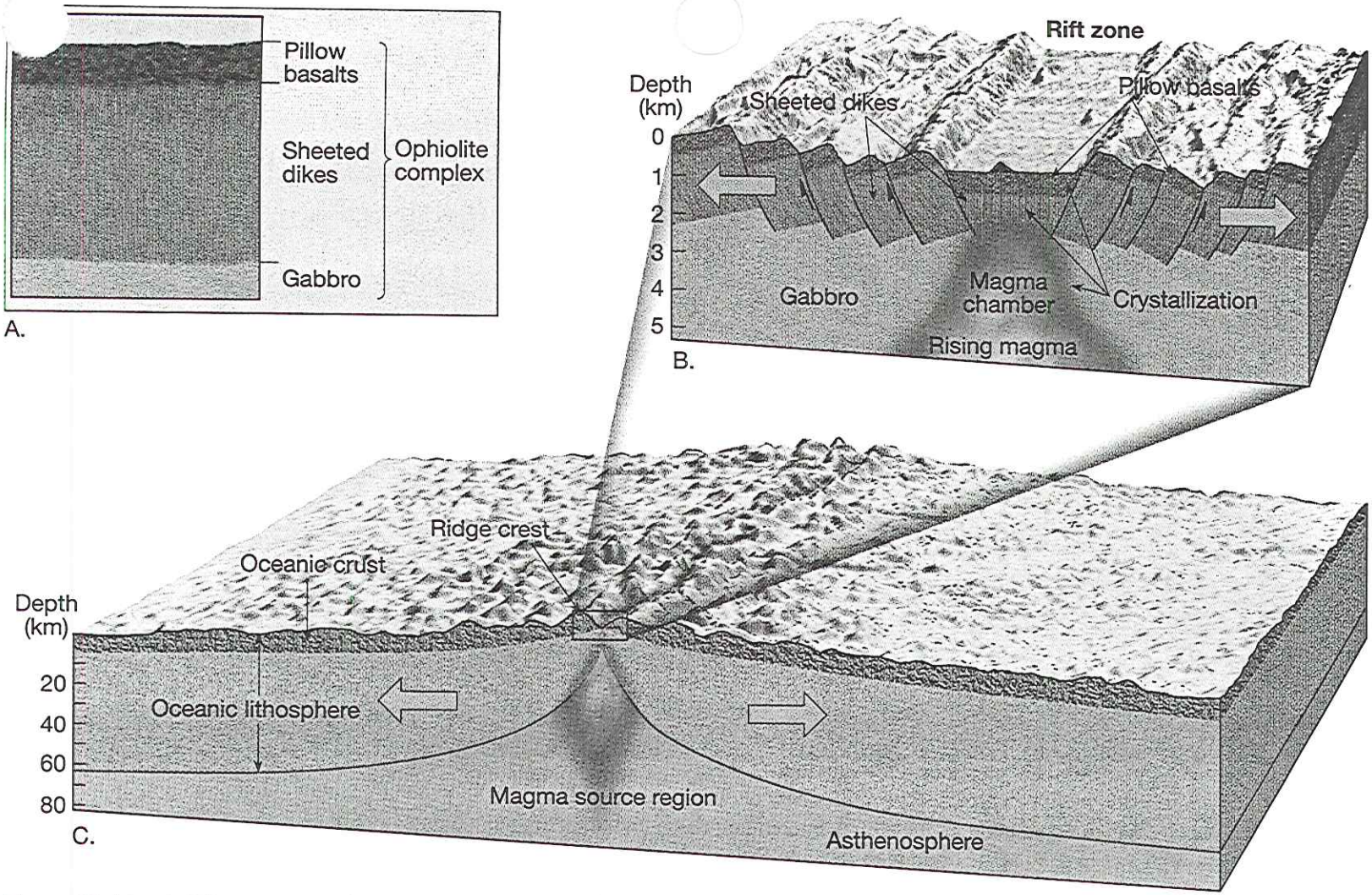


Figure 19.14 **A.** The structure of oceanic crust is thought to be equivalent to the ophiolite complexes that have been discovered elevated above sea level in such places as California and Newfoundland. **B.** The formation of the three units of an ophiolite complex in the rift zone of an oceanic ridge. **C.** Diagram illustrating the site where new ocean crust is generated.

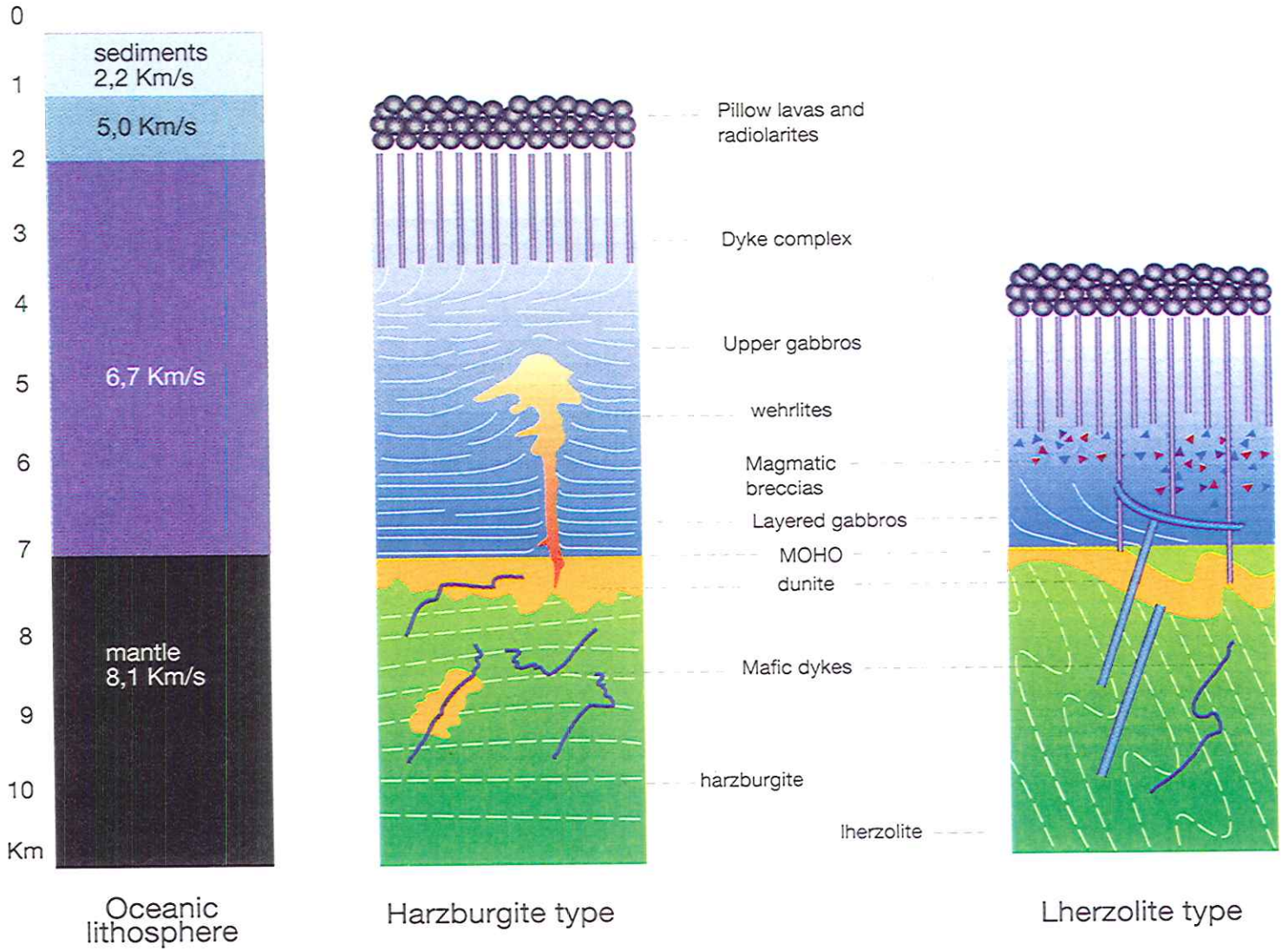


**Figure 5.8**
Columns comparing the structure of the oceanic crust as defined seismically with the two main types of ophiolites: the harzburgite type as illustrated by the Oman ophiolites and the lherzolite type, by the Trinity ophiolites of California. (After F. Boudier and A. Nicolas 1985, Earth Planet. Sci. Lett., 76, 84–92)

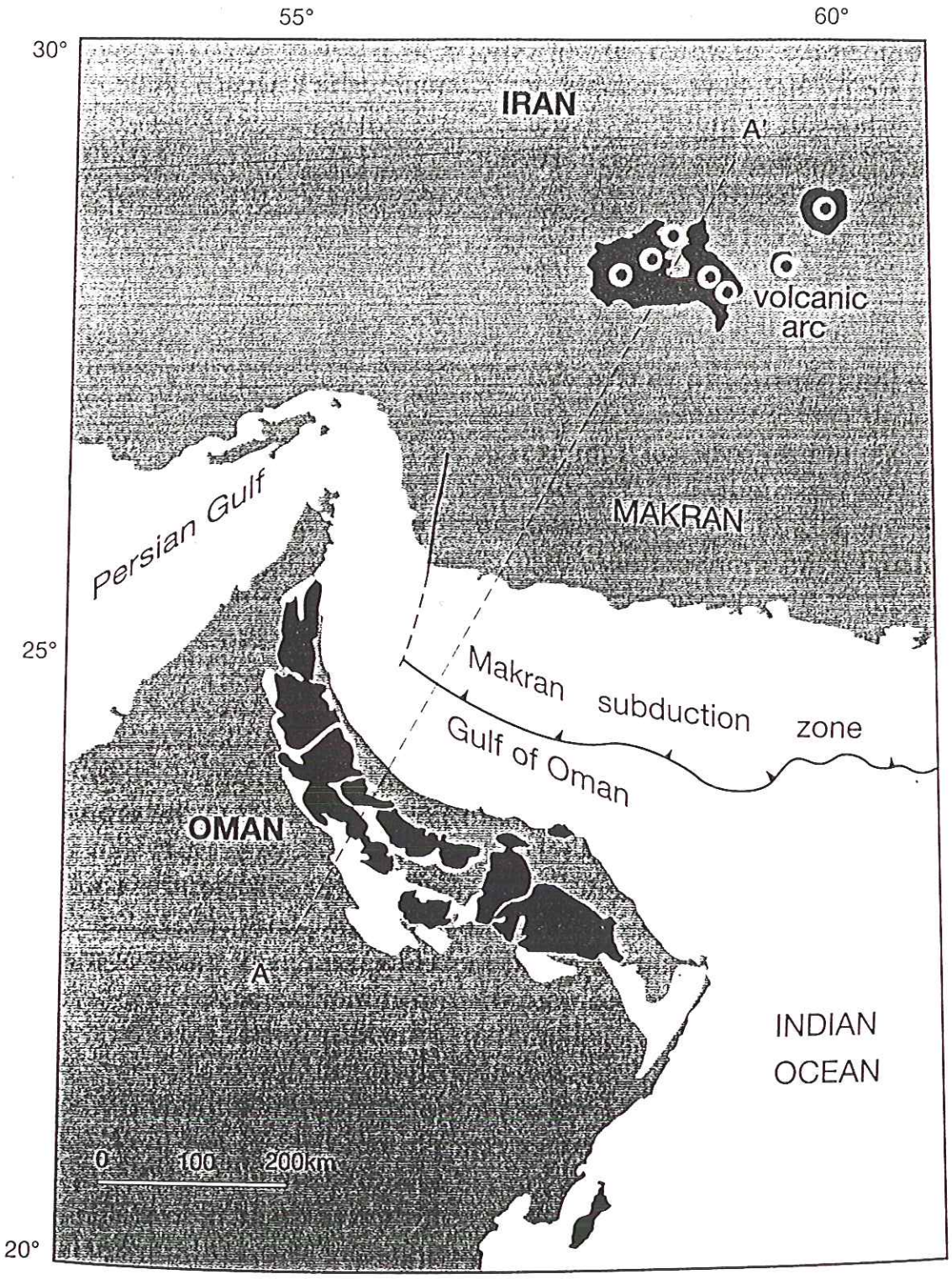


**Figure 5.3**
The Oman ophiolites (*deep blue*) and the Hawasina sediments (*yellow*), both thrust together onto the Arabian Shield. To the NNE, in the Gulf of Oman, the front of the Makran subduction zone is shown by the *thrust symbol.* Still farther north, in Iran, there is a volcanic arc genetically related to this subduction. Section *A-A'* corresponds to **e** in Fig. 5.4

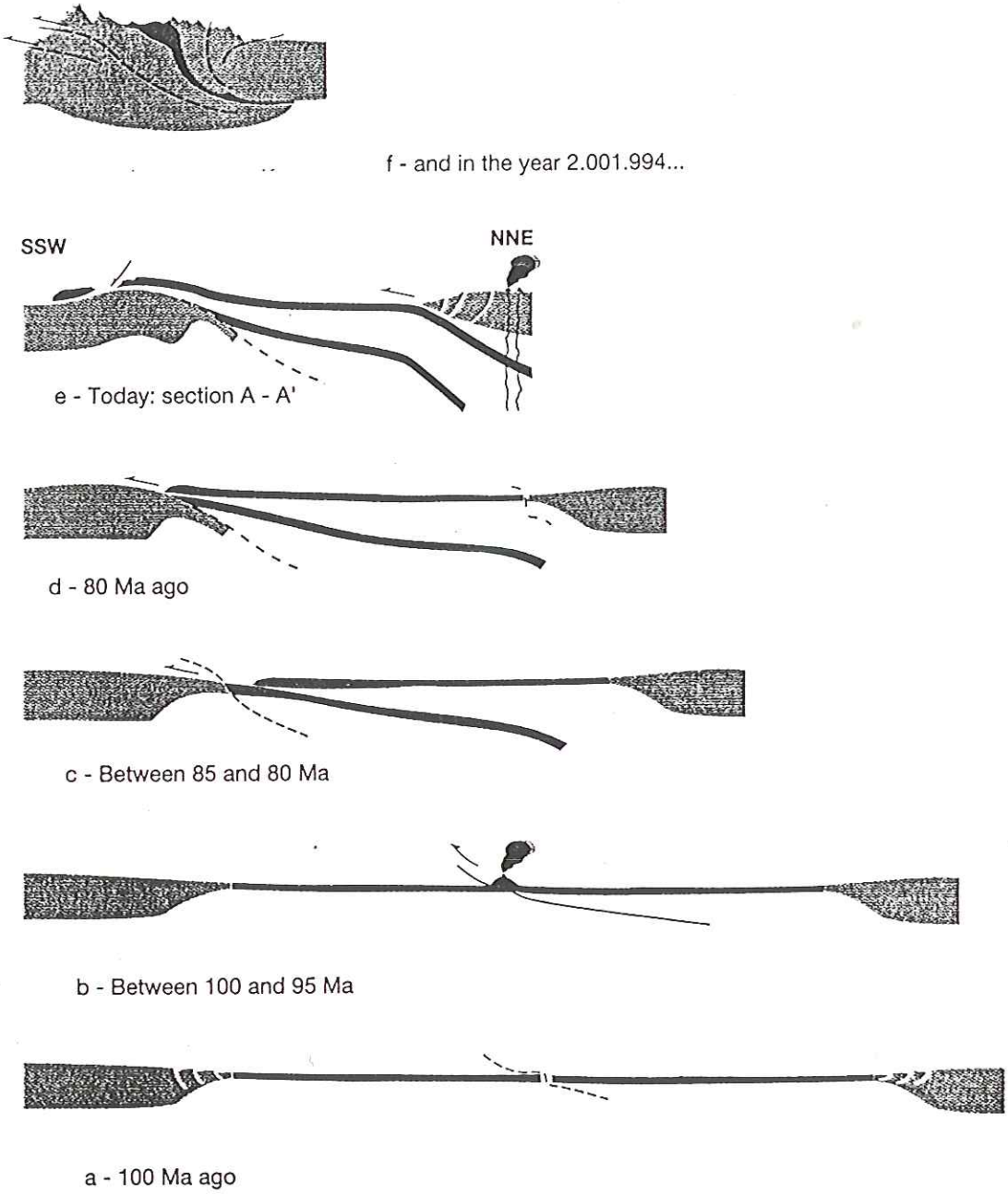


**Figure 5.4 a–f**
Profiles illustrating the obduction of the Oman ophiolites from their formation about 100 Ma ago (**a**) to the present stage (**e**), along line A-A' in Fig. 5.3. (**f**) The collision about 2 Ma from now in the future is shown. (After A. Nicolas 1989, Structures of ophiolites and dynamics of oceanic lithosphere, Kluwer Ed., 367 p.)

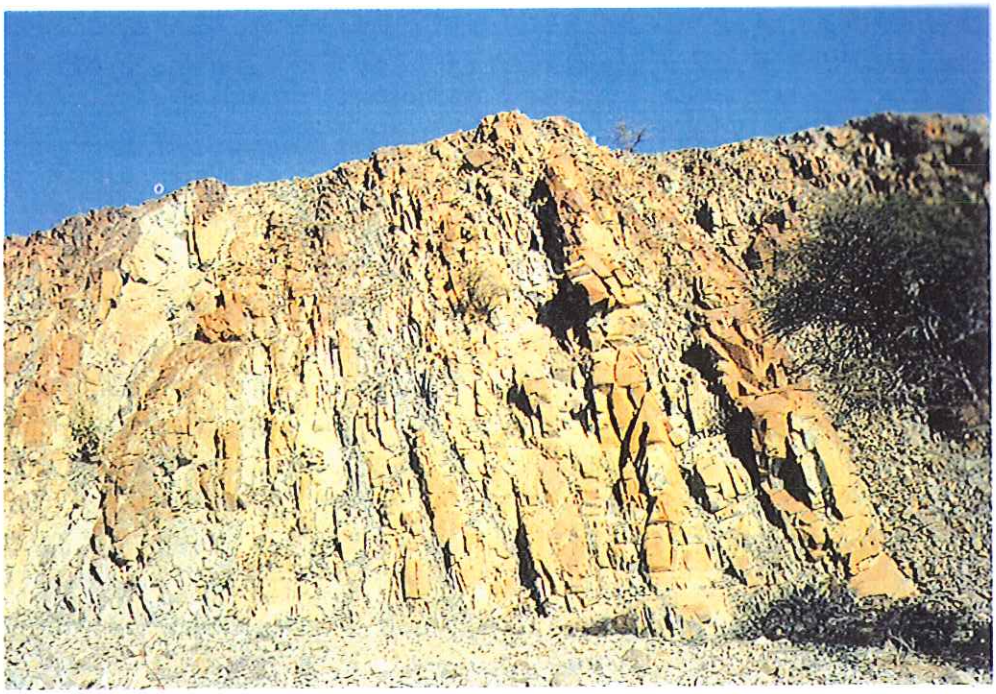

c

d

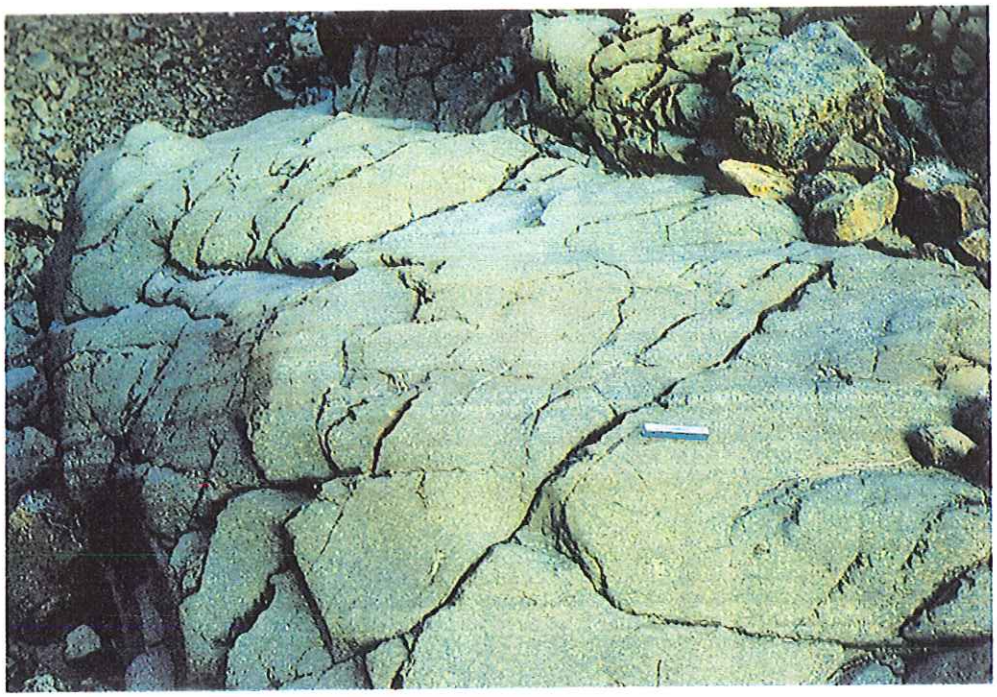

a

b

Figure 19.15 Ancient pillow lava at Trinity Bay, Newfoundland. (Photo courtesy of the Geological Survey of Canada, photo no. 152581)

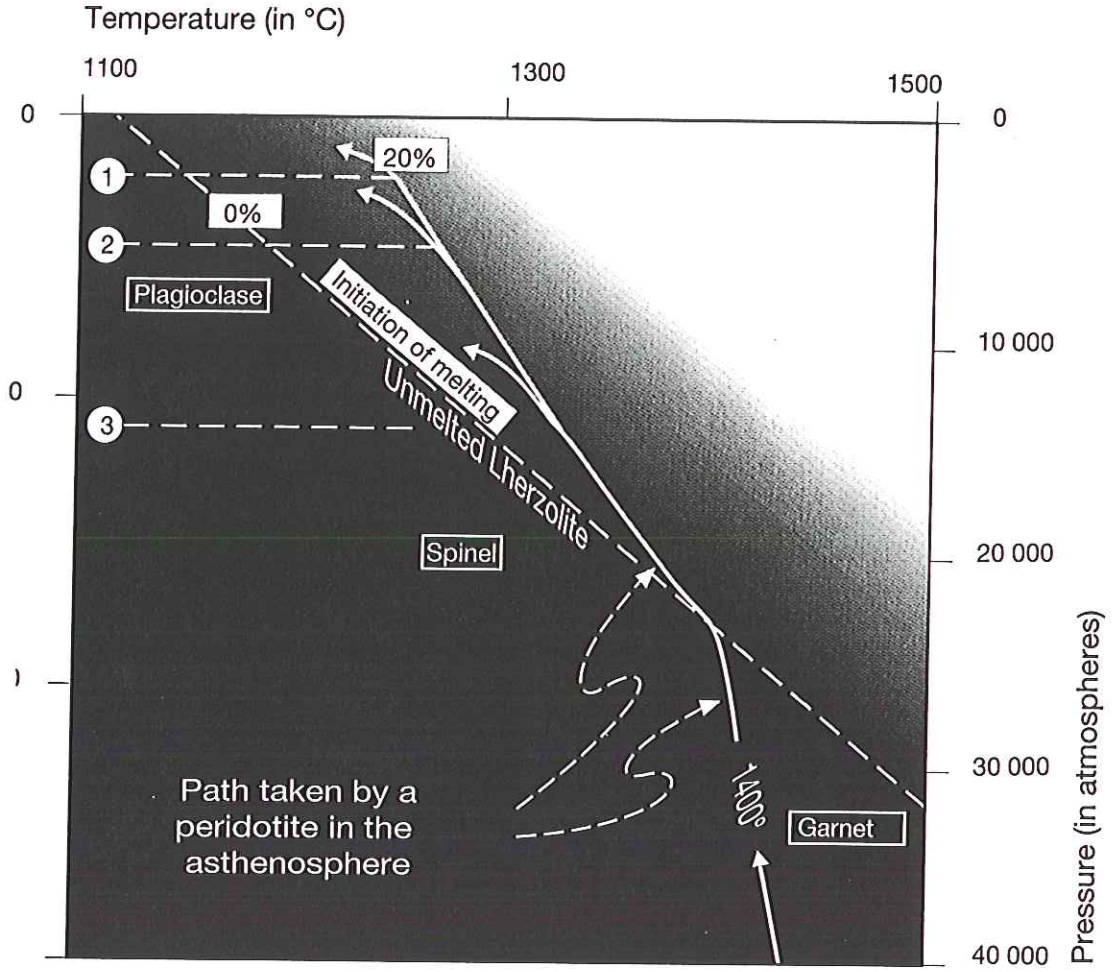


**ıre 6.6**

ɡram of the evolution of temperature and melting of a mantle peridotite dur-ascent to the surface. The trajectory follows the *white arrows from bottom to top.* ıg within the dry asthenosphere (*dark red*), the peridotite starts to melt when osses into the lighter-coloured areas. The increasing degree of melting is :ated by *increasingly lighter red colour.* The diagram contains two other pieces formation: In the "solid" domain (*dark red*), depending on the depth, the lotite may contain garnet (below 75 km), spinel (30–75 km), or plagioclase ve 30 km). *1*, *2*, and *3* correspond respectively to three possible trajectories, nding on the depth at which the rising peridotite becomes incorporated in thosphere (cf. Chap. 8)

a

Fast ridge
Extraction of 20% basalt
Normal oceanic crust

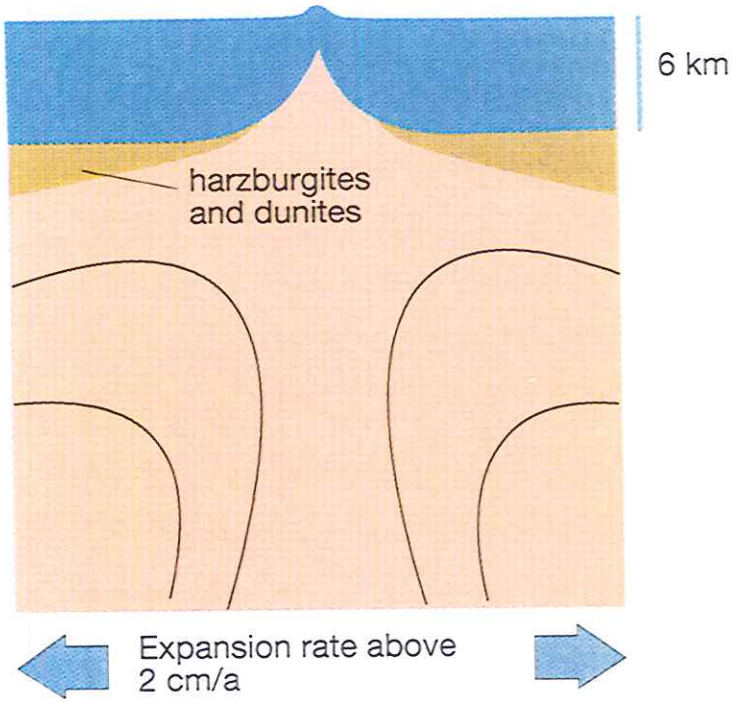


b

Slow ridge
Extraction of 10% basalt
Thin or abnormal oceanic crust

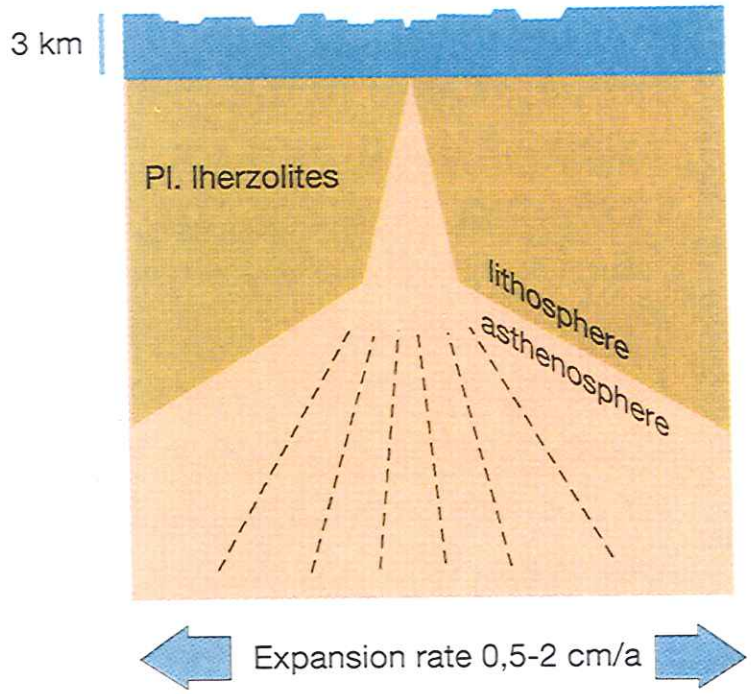

The best exposed is in Oman — 500 km long

ophiolite — ophis — Greek — snake
lithos - rock

"snake rock" — because of scaly appearance and greenish color — predominance of olivine — itself named after it's color.

also occurrences in Cyprus, Turkey, Cuba, Newfoundland, Philippines, New Guinea, New Caledonia, California (John McPhee)

Rate of basalt generation on all ridges is ~ 16 km³/yr
(many times that on continents)

In detail the degree of partial melting (10% – 20%) and the crustal thickness depend (weakly) upon the spreading rate.

Seismic evidence (on fast-spreading ridges) shows that the axial magma chamber (AMC) is very shallow

What does T(z) look like at deeper depths? Uncertainties increase. Several questions:

(1) whole mantle or lower vs. upper mantle convection

Presence of predominantly Fe molten core (2900 km depth) provides a constraint

Solid inner core 5100 km depth

Traditional estimate for $T_{center\ of\ \oplus}$ is $\sim 4000^\circ C$.

Newer ideas, based on high-P studies of $T_{melt}$ for Fe say may be as high as $6500^\circ C$

By comparison $T_{surface\ of\ Sun} = 5800^\circ C$

We know the latter very well from spectrum of sunlight.

What is the source of the $\oplus$'s internal heat?

(1) conversion of kinetic energy of colliding planitesimals into heat

(2) iron catastrophe — conversion of gravitational potential energy to

(3) continuing solidification of inner core

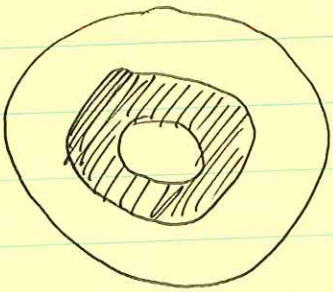

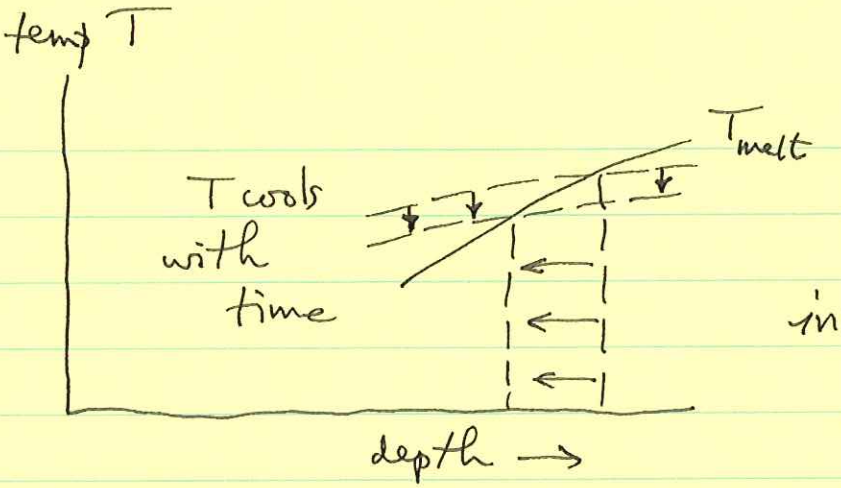


inner core grows with time as ⊕ cools off.

Very slow process — will take several b.y. more to solidify
~ growth rate ~ 1 mm/yr.

Responsible for stirring of fluid core — mechanism for ⊕'s magnetic field.

Fluid core is Fe + 10% light alloy — latter is left behind — rises to top.

(4) radioactivity:

| | | |
|---|---|---|
| potassium | K | all have ~ b.y. half-lives |
| uranium | U | |
| thorium | Th | |

When they decay heat is released.

Concentrated in (enriched) continental crustal rocks

This was a more important source of heat in the past.

Early ⊕ [illegible] b.y. ago
(say 3–4 b.y. ago)
was convecting more vigorously.
Plate tectonics more rapid,
lithosphere thinner, ⊕ hotter.

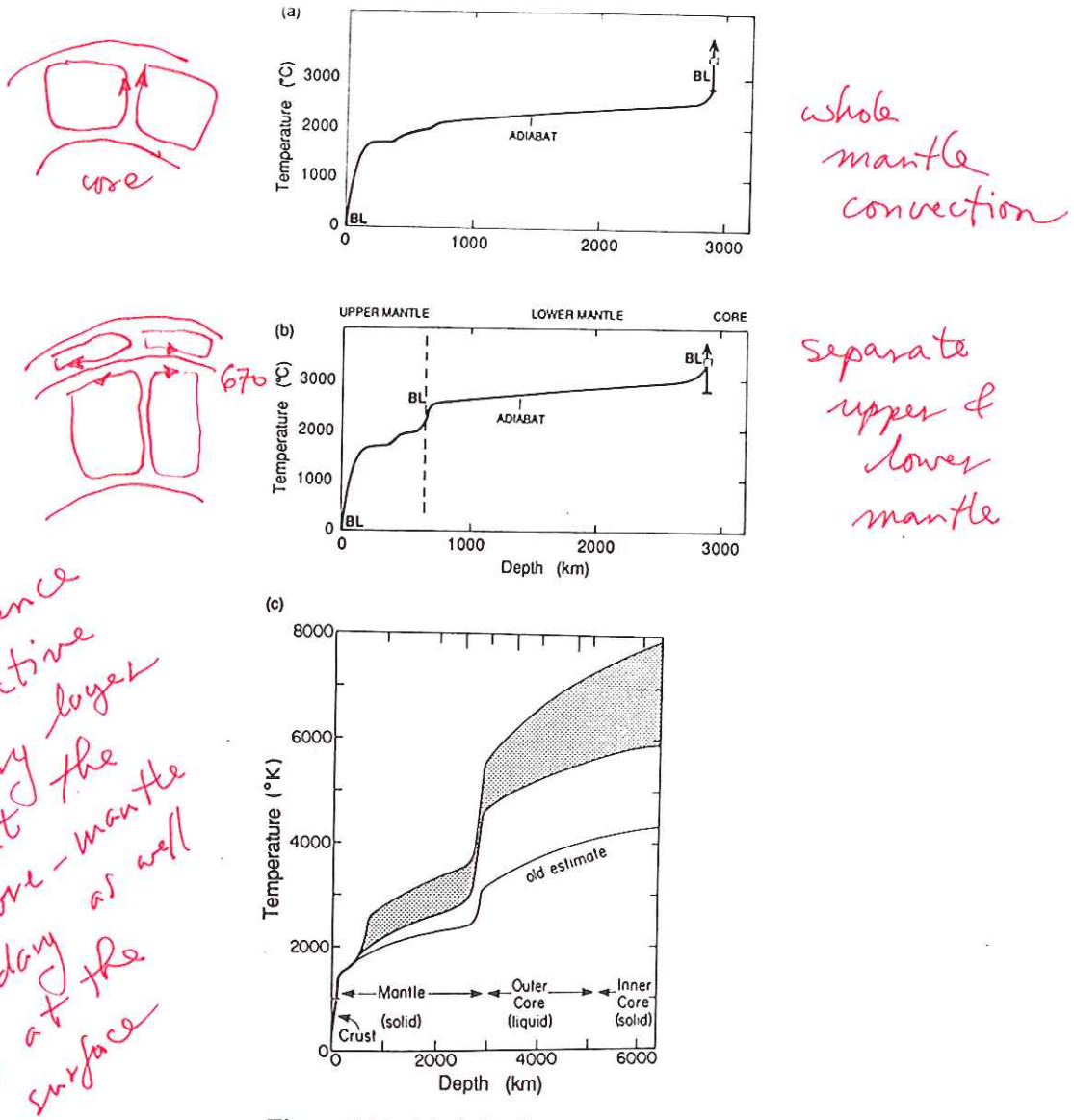


Figure 7.16. Models of temperature profiles in the earth. (a) Mantle adiabat with a thermal boundary layer (BL) at the surface and at the core–mantle boundary. (b) Mantle adiabat with a thermal boundary layer (BL) at both the top and the bottom of the lower mantle. The dashed line indicates a chemical and dynamic boundary between the upper and lower mantle, which are assumed to be separate systems. For (a) and (b) the temperature at the core–mantle boundary is assumed to be in the range 2900–3200°C. (c) An alternative estimate of the temperature in the earth based on high-pressure (over 1000 GPa) and high-temperature (700–6700°C) experiments on iron. The shaded region reflects the uncertainty in the temperature of the core (6600 ± 1000°C at the centre of the earth). The old estimate is similar to profiles shown in (a) and (b) and is typical of temperature profiles proposed prior to 1987. (From Jeanloz and Richter 1979 and Jeanloz 1988.)

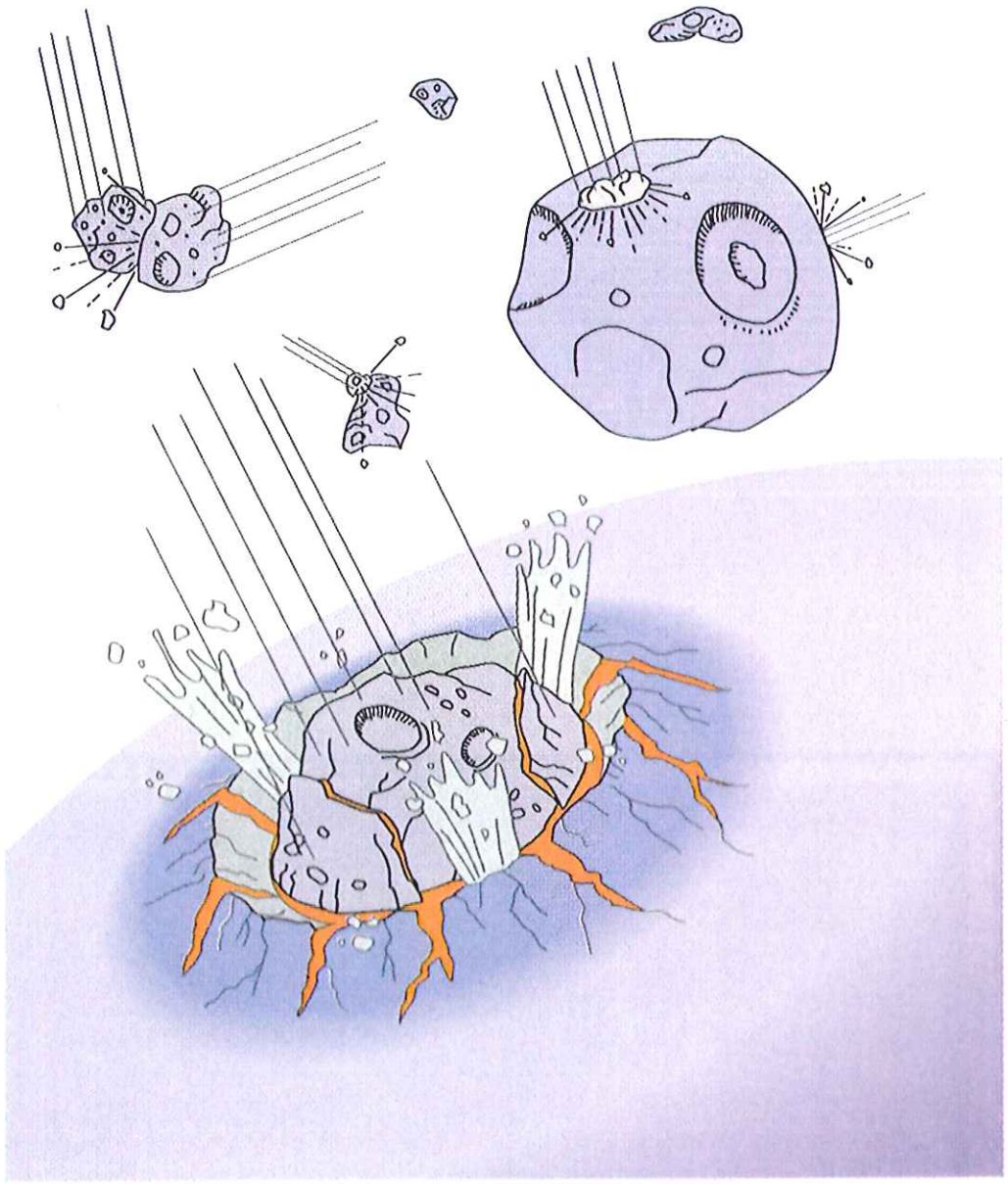

**FIGURE 8.1** Four and a half billion years ago a lot of debris, ranging in size from dust to asteroids, still orbited the young Sun. Collisions between these materials, called *planetesimals*, were frequent. As planetesimals gradually accumulated to form larger bodies, these developed stronger gravitational fields and began to attract more particles from nearby space. Each impact added heat to the planet and buried earlier hot rocks under a new blanket of debris. According to some estimates, the Earth could have grown to full size by this process of accretion in a few tens of millions of years. Long before it did, the planet had become so hot that its outer region melted completely to form a global-scale ocean of magma.

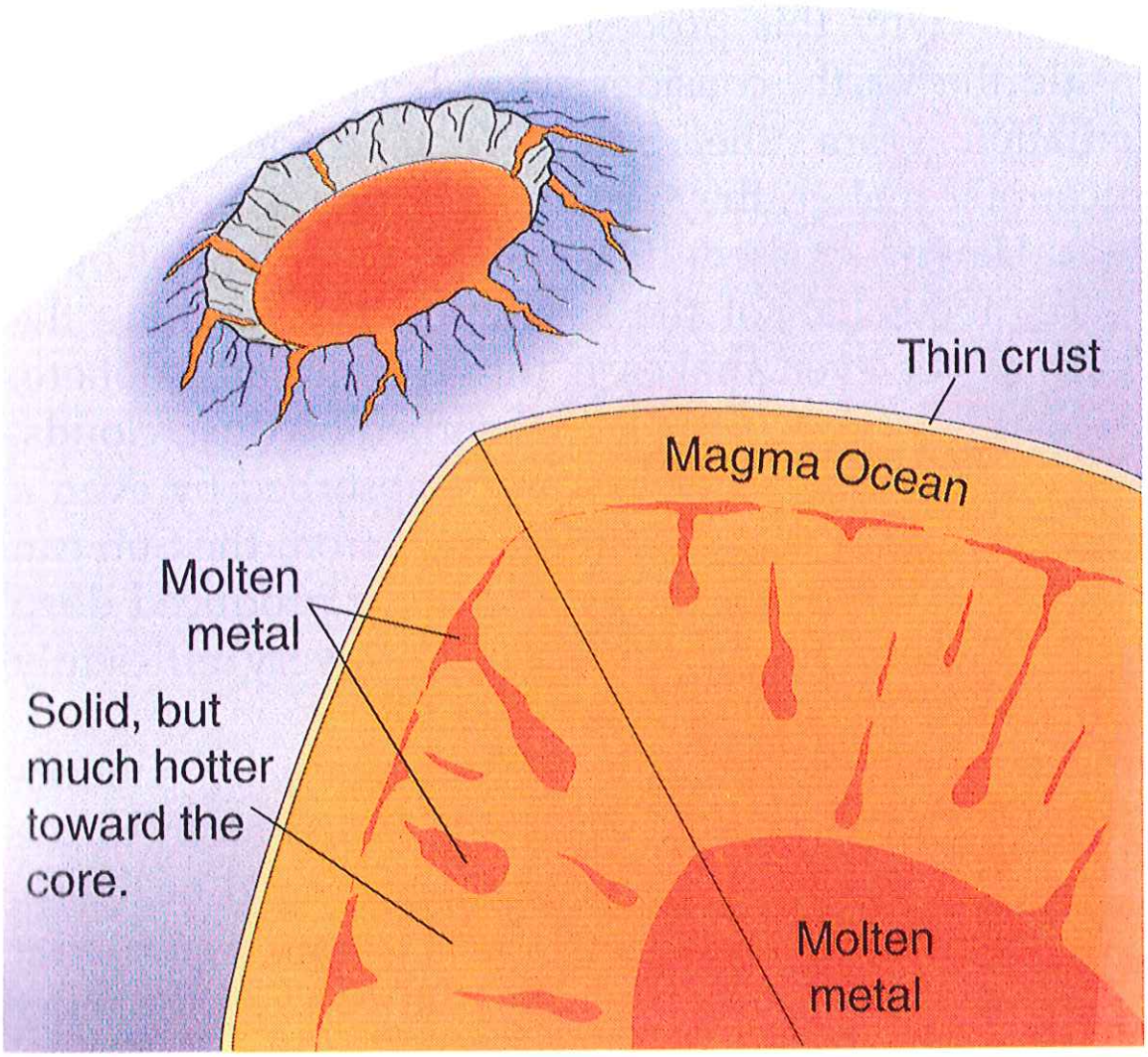


**FIGURE 8.2** Liquid iron/nickel, separated from the outer portion of the young Earth, gradually settled toward the center of the planet because of its high density. As it "fell" through the mantle and had to overcome its viscosity, some of the metal's energy of motion was converted into heat. This "iron catastrophe" was a second source of gravitational heating in the young Earth.

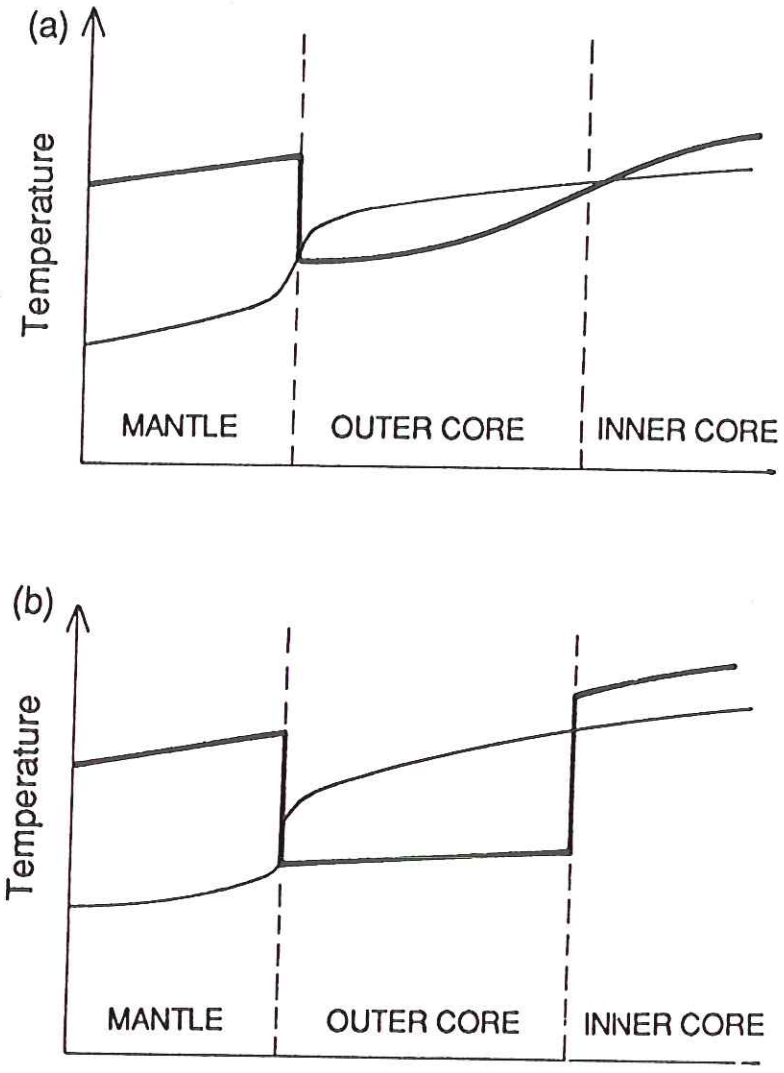


Figure 7.22. Schematic of possible melting temperatures for the mantle and core and the actual temperature profile. Heavy line, melting curve; lighter line, actual temperature profile. (a) Chemically homogeneous core. As the core cools, the inner core grows. (b) The inner and outer core have different chemical compositions and hence different melting temperatures. An outer core composed of an Fe–S or Fe–O alloy would have a much lower melting temperature than a pure iron inner core.

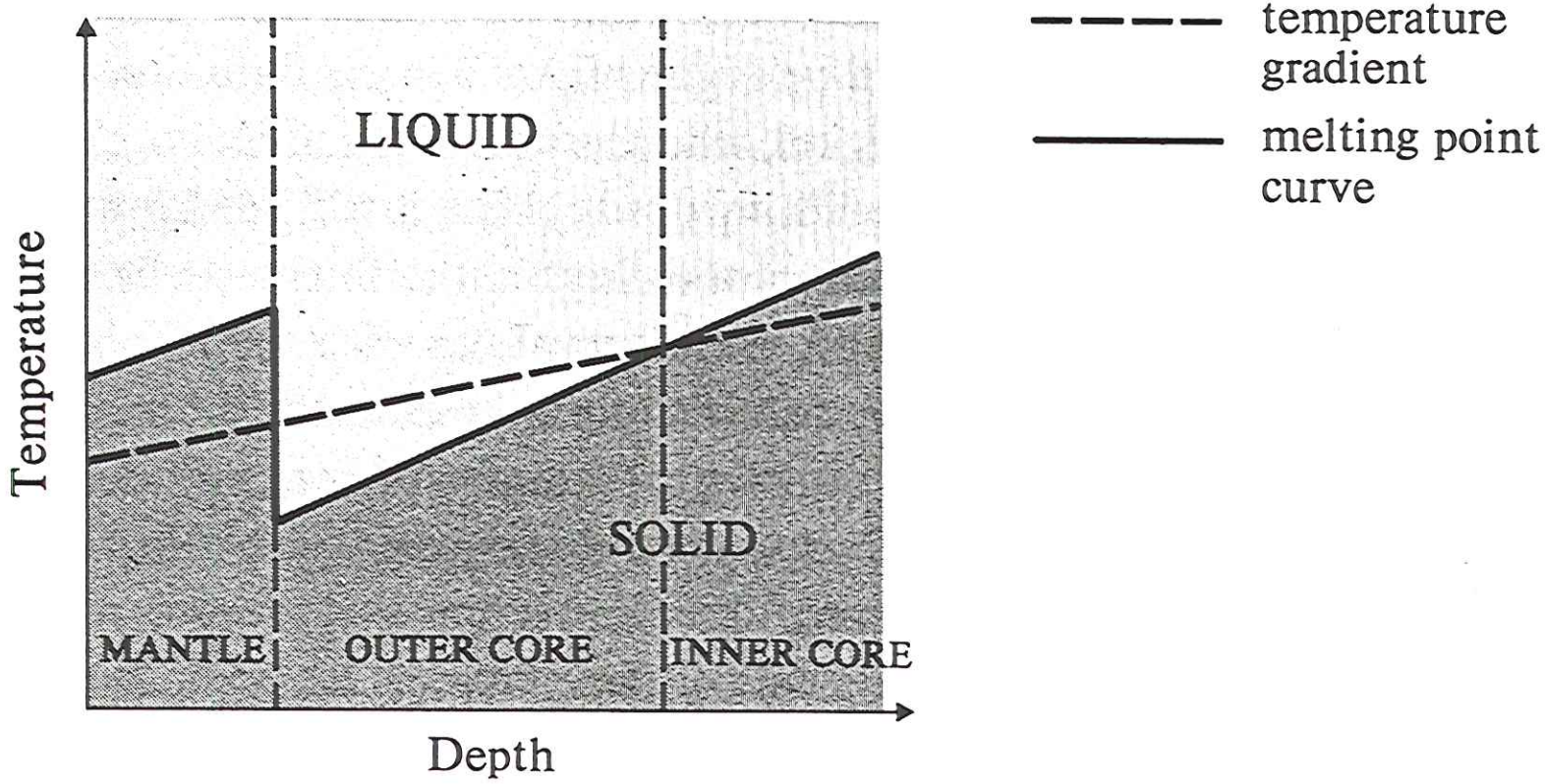
LIQUID
SOLID
MANTLE
OUTER CORE
INNER CORE
Temperature
Depth
temperature gradient
melting point curve

(a)

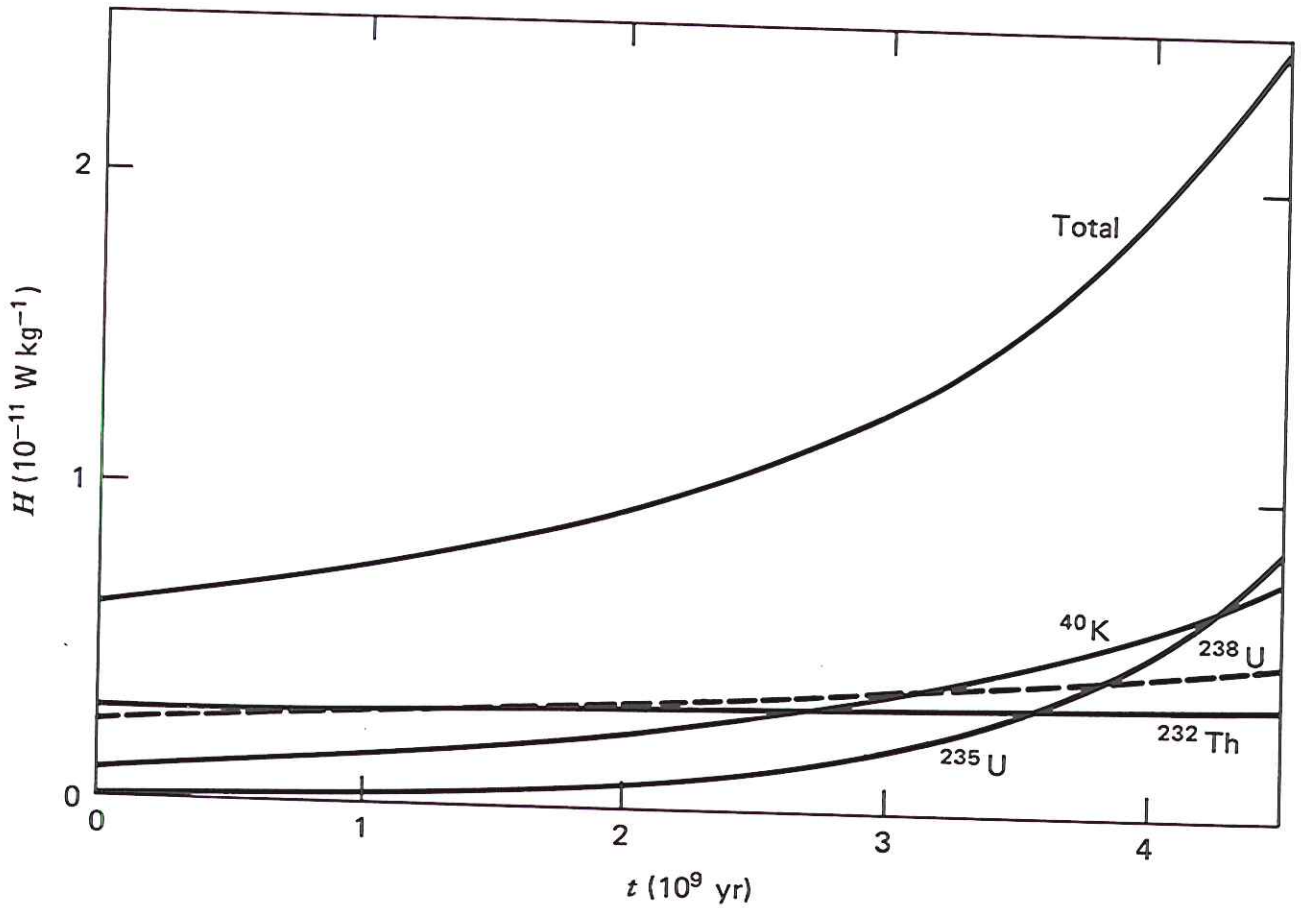


**Figure 4-4** Mean mantle heat production rates due to the decay of the radioactive isotopes $^{238}U$, $^{235}U$, $^{232}Th$, and $^{40}K$ as functions of time measured back from the present.

at 1 atm pressure

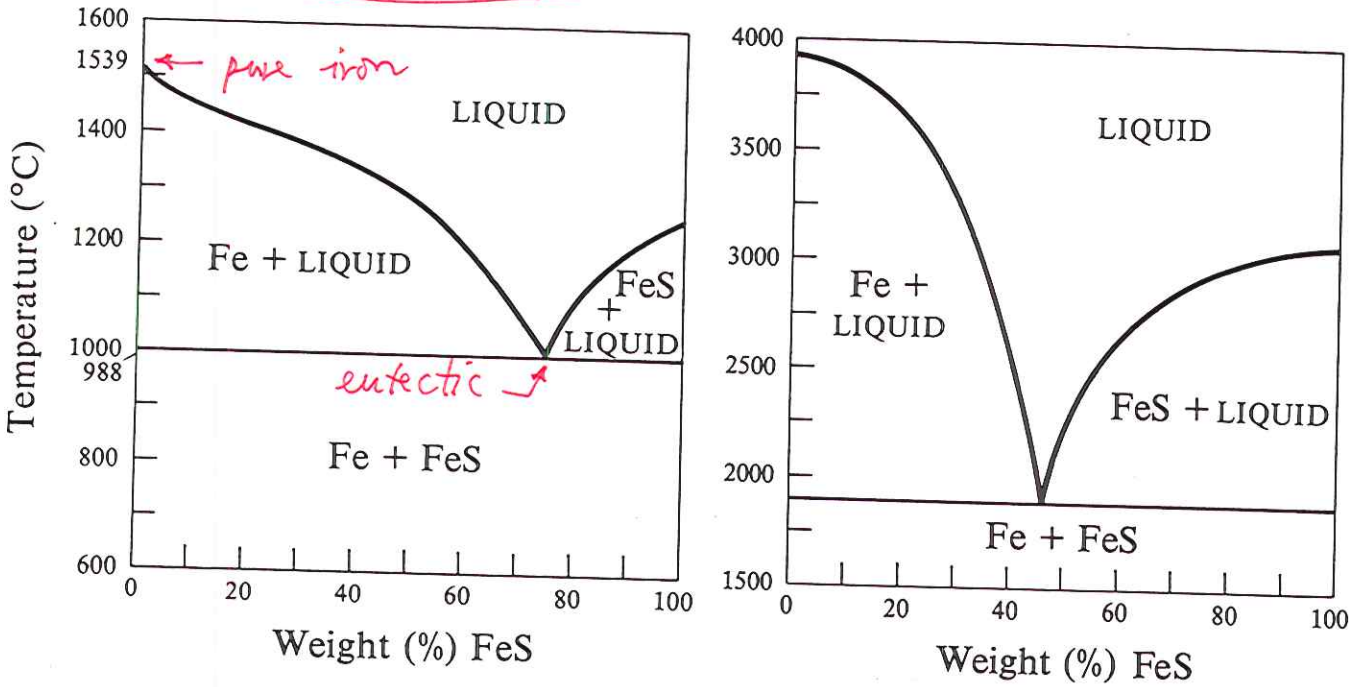


**Figure 6.6** Melting relations of Fe–FeS mixtures (a) at 1 atm pressure and (b) extrapolated to the pressure of the core–mantle boundary (1·4 Mbar). (Data from Usselman 1975.) Note that the two temperature scales are different.

light alloying element in Fe core — possibly sulfur — lowers melting temperature

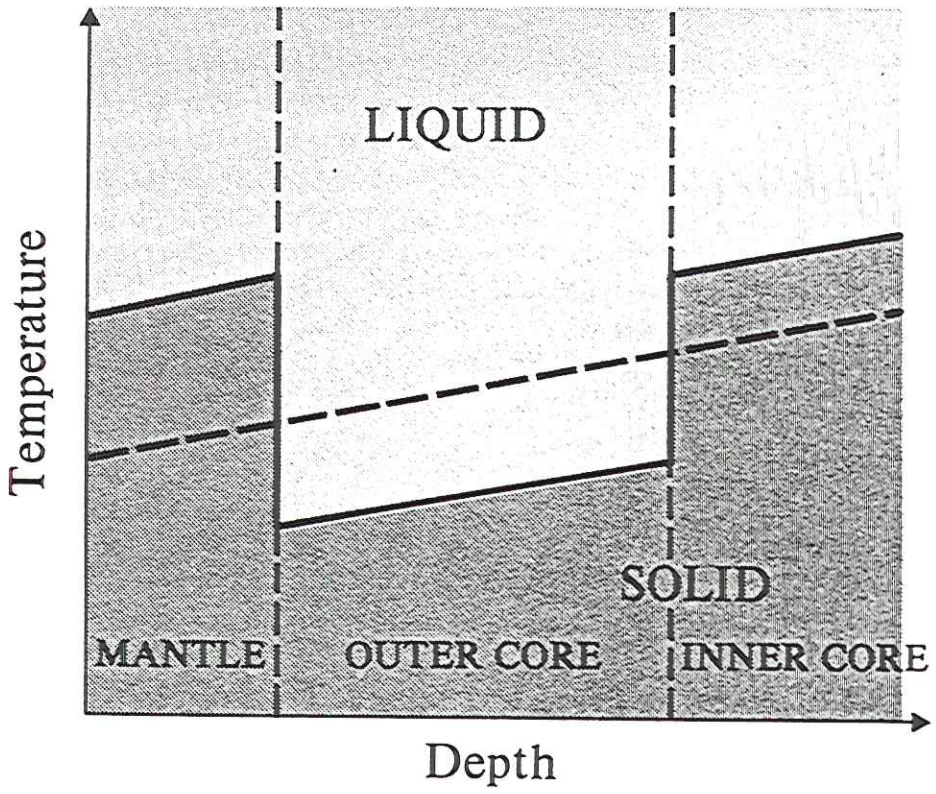


(c)

possible thermal gradient

melting point curve

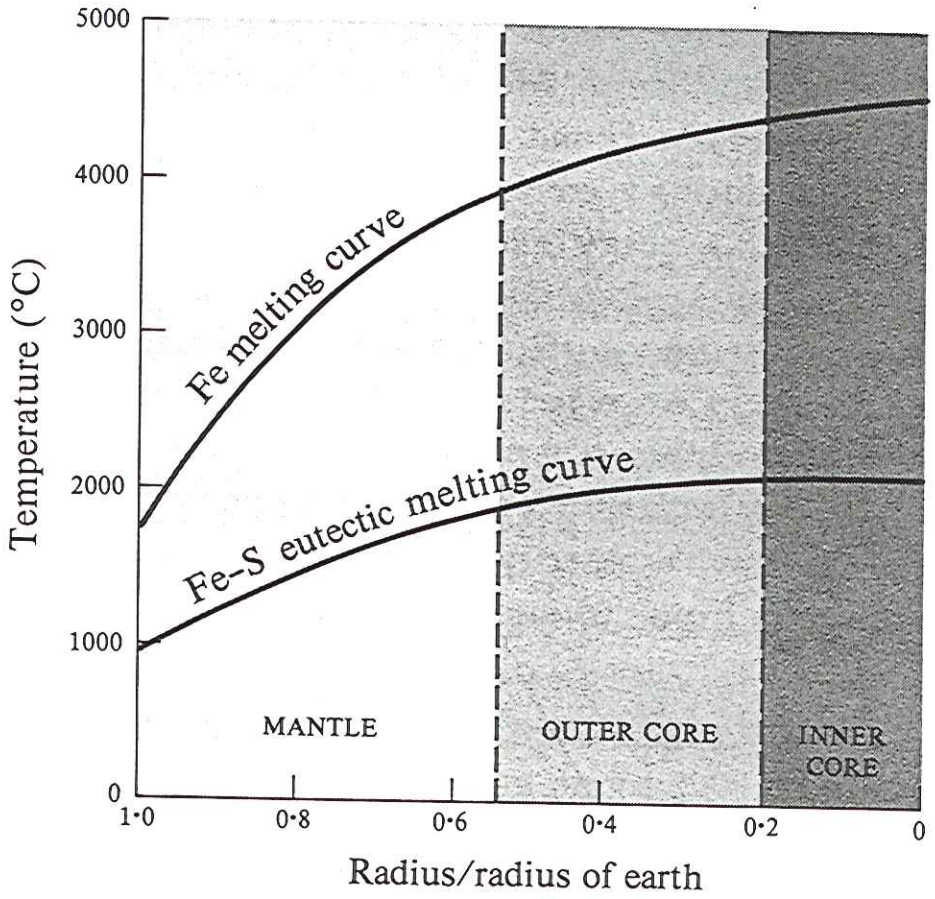


**Figure 6.7** Variation of Fe and Fe–S eutectic melting curves in the Earth. Note from Fig. 6.6 that though the eutectic composition is 27% S (75% FeS) at the surface, it changes to 17.5% S (48% FeS) at the core/mantle boundary and to 15% S (41% FeS) at the inner core/outer core boundary. The two curves provide limits on the temperature in the outer core. (Data from Usselman 1975.)

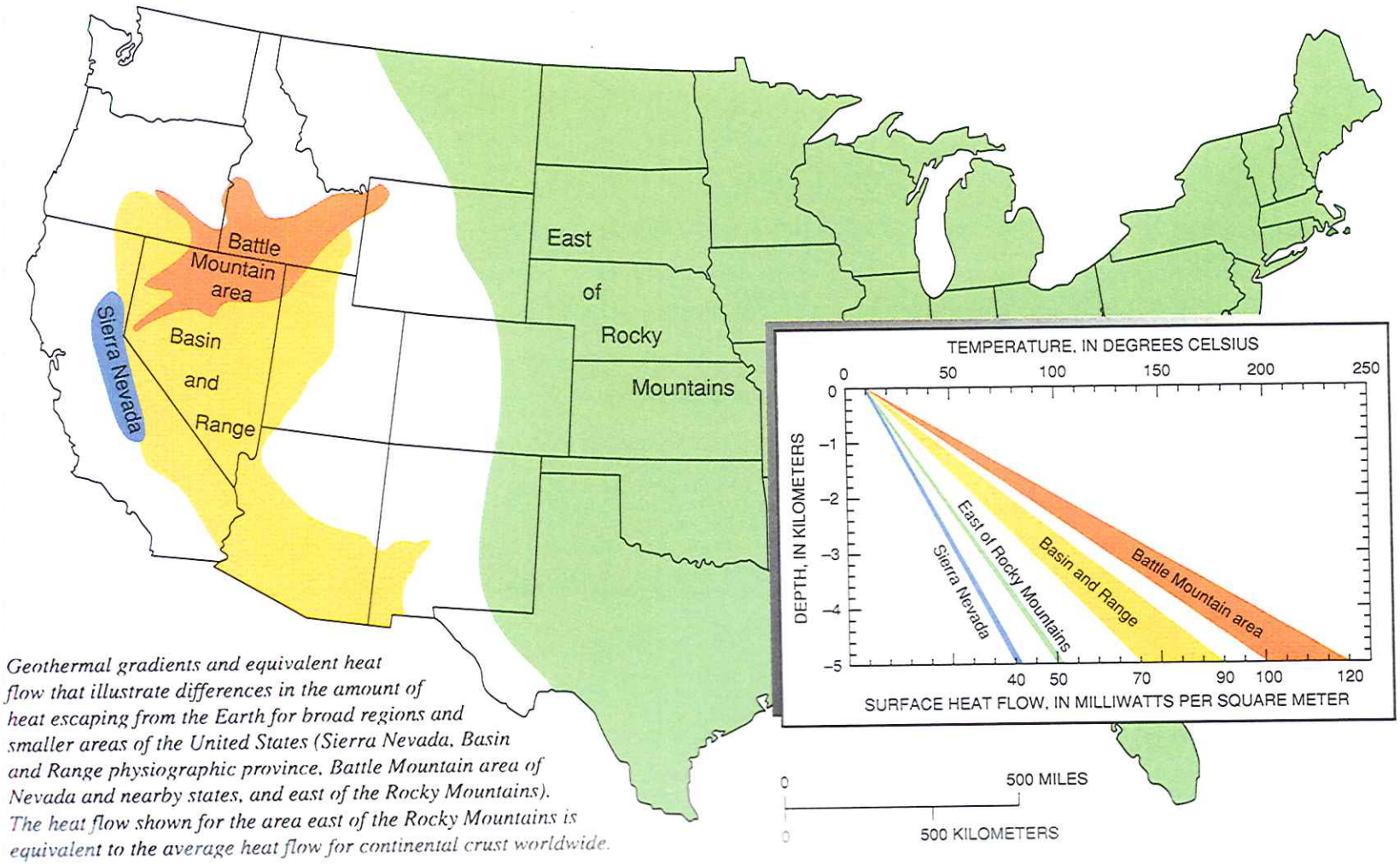


*Geothermal gradients and equivalent heat flow that illustrate differences in the amount of heat escaping from the Earth for broad regions and smaller areas of the United States (Sierra Nevada, Basin and Range physiographic province, Battle Mountain area of Nevada and nearby states, and east of the Rocky Mountains). The heat flow shown for the area east of the Rocky Mountains is equivalent to the average heat flow for continental crust worldwide.*

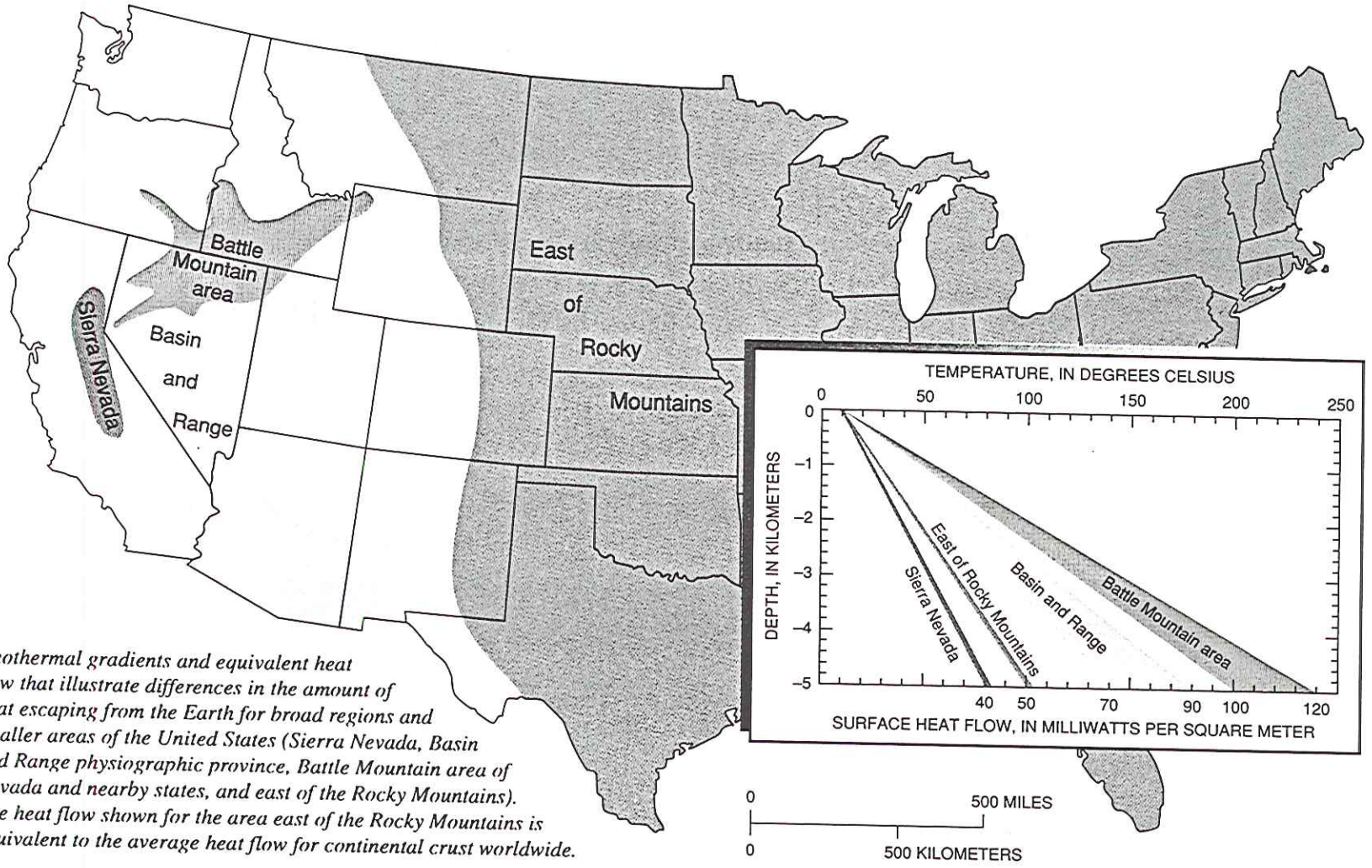


*Geothermal gradients and equivalent heat flow that illustrate differences in the amount of heat escaping from the Earth for broad regions and smaller areas of the United States (Sierra Nevada, Basin and Range physiographic province, Battle Mountain area of Nevada and nearby states, and east of the Rocky Mountains). The heat flow shown for the area east of the Rocky Mountains is equivalent to the average heat flow for continental crust worldwide.*

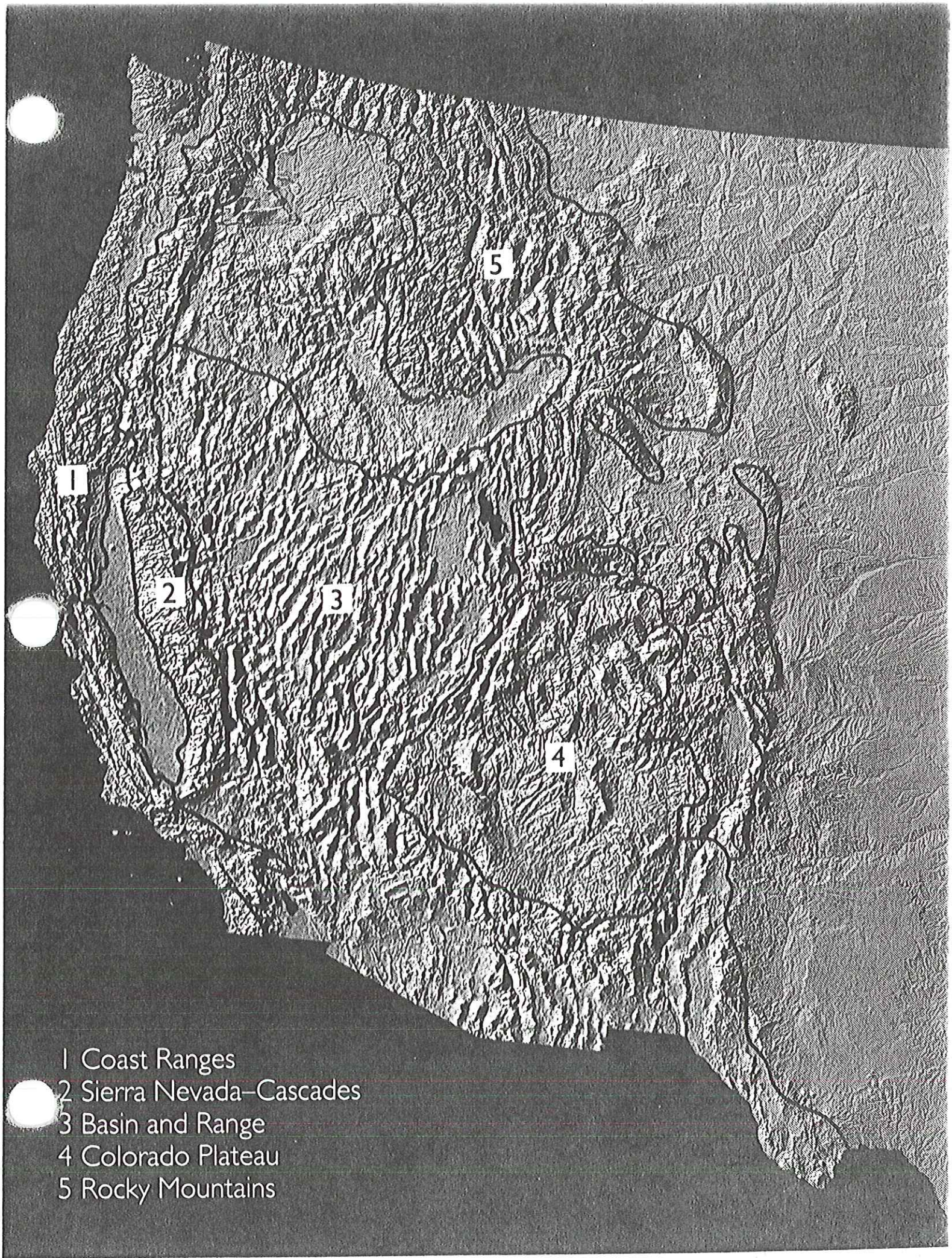


1 Coast Ranges
2 Sierra Nevada–Cascades
3 Basin and Range
4 Colorado Plateau
5 Rocky Mountains

Heat — a form of energy — measured in joules

$$1\ J = 1\ \frac{kg\ m^2}{s^2}$$

Power — rate at which energy is produced or consumed, etc. — measured in watts

$$1\ W = 1\ \frac{J}{s}$$

Calorie: amount of heat required to raise temperature of 1 gm of $H_2O$ by 1°C.

$$1\ \text{calorie} = 4.184\ J$$

Conductive heat flow within the Earth

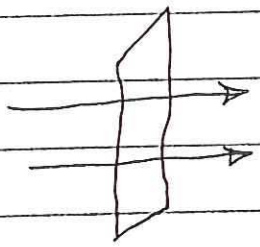


1m x 1m area

$$\frac{J}{m^2 s} = \frac{W}{m^2}$$

$$1\ \frac{mW}{m^2} = \frac{1}{1000}\ \frac{W}{m^2}$$

Mean surface heat flow: $\bar{q} = 60\ mW/m^2$

$\bar{q} \times$ (surface area of $\oplus$) $= 3 \cdot 10^{13}\ W$

Heat conduction is governed by Fourier's law:

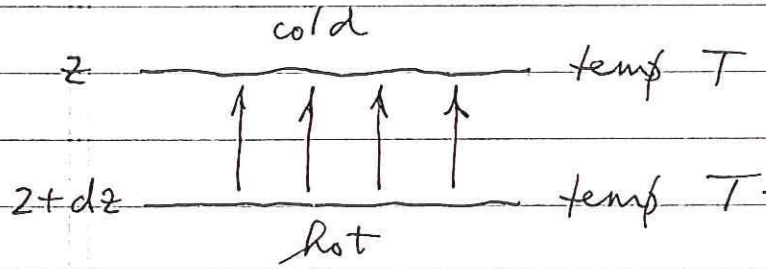


$$q = \kappa \left[ \frac{T + dT - T}{z + dz - z} \right] = \kappa \frac{dT}{dz}$$

heat flow = thermal conductivity × temperature gradient

Thermal conductivity $\kappa$ : $\frac{W/m^2}{^\circ C/m} = \frac{W}{m\,^\circ C}$

| material | $\kappa$ (W/m °C) |
|---|---|
| Cu | 400 |
| Al | 240 |
| Fe | 80 |
| dry rock | 3 |
| water | 0.6 |
| soil | ~ 0.6 |
| styrofoam | 0.03 |

conductors

insulators

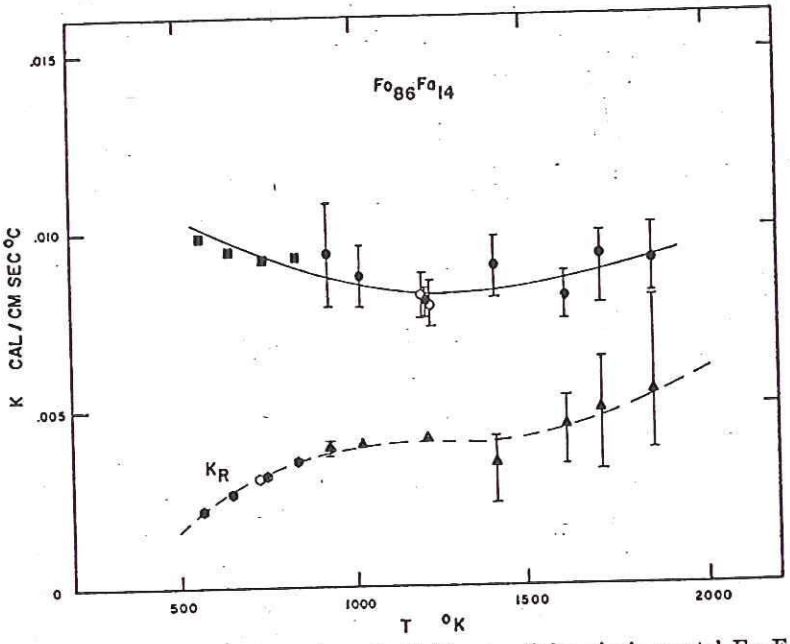


Fig. 5b. Total and radiative thermal conductivities in olivine single crystal $Fo_{86}Fa_{14}$. Open circles are points measured at descending temperature. Solution below 900°K are obtained by using assumed values of $\kappa_L$.

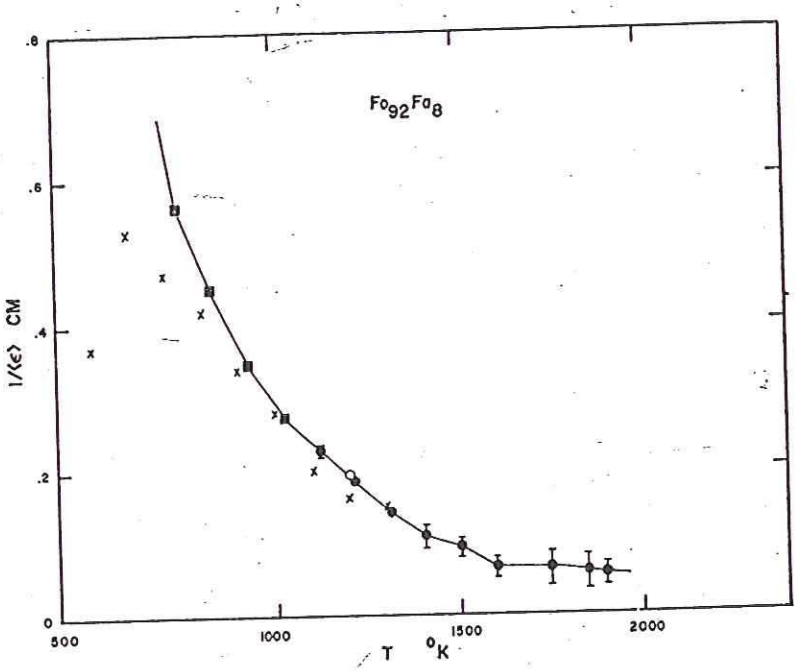


Fig. 6a. Photon mean free path in olivine single crystal $Fo_{92}Fa_8$. The open circle is a point measured at descending temperature. Solutions below 1100°K are obtained by using assumed values of $\kappa_L$. The crosses are data of *Fukao et al.* [1968] for a crystal of olivine composition $Fo_{88}Fa_{12}$.

Solar constant : 1370 $W/m^2$

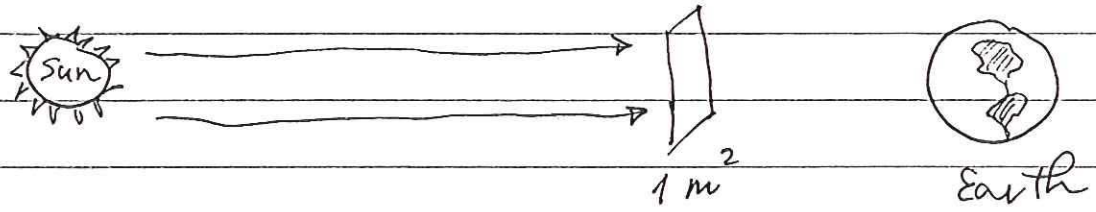


Averaged over ⊕ surface : $\frac{1370}{4} = 340 \frac{W}{m^2}$

Total solar energy striking the ⊕ :

$340 \times 4\pi (\text{radius})^2 = 1.7 \cdot 10^{17}$ W

Albedo : 30% reflected back into space

Solar energy incident at ⊕ surface
= 4000 × (total conductive heat flow from interior)

Typical geotherm at ⊕ surface : 20 °C/km

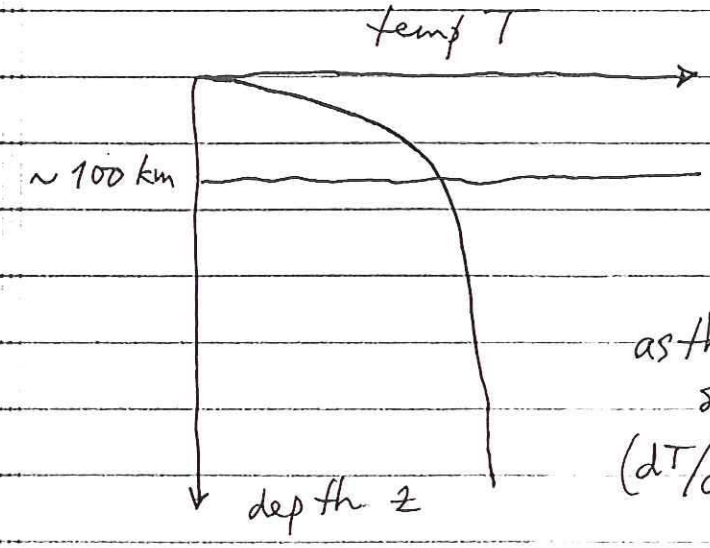


lithosphere : dominated by conduction
$dT/dz \sim 20$ °C/km

asthenosphere : dominated by subsolidus convection
$(dT/dz)_{adiabatic} \sim 0.6$ °C/km

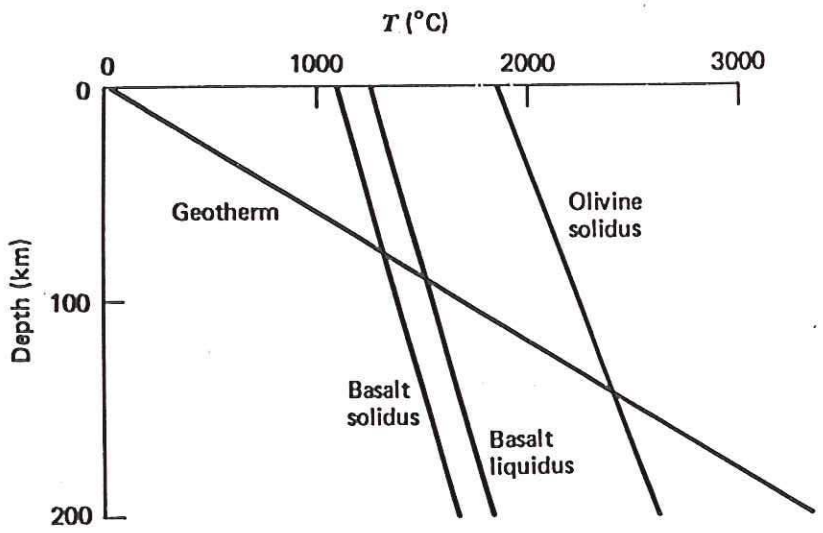


**Figure 4-8** Temperature as a function of depth within the earth assuming heat transport is by conduction (conduction geotherm). Also included are the solidus and liquidus of basalt and the solidus of peridotite.

FIGURE 8.12 Estimated average geotherms in continental and oceanic lithosphere. The convecting mantle is nearer to the surface in the ocean basins than under the continents, so high temperatures are reached at relatively shallow depths.

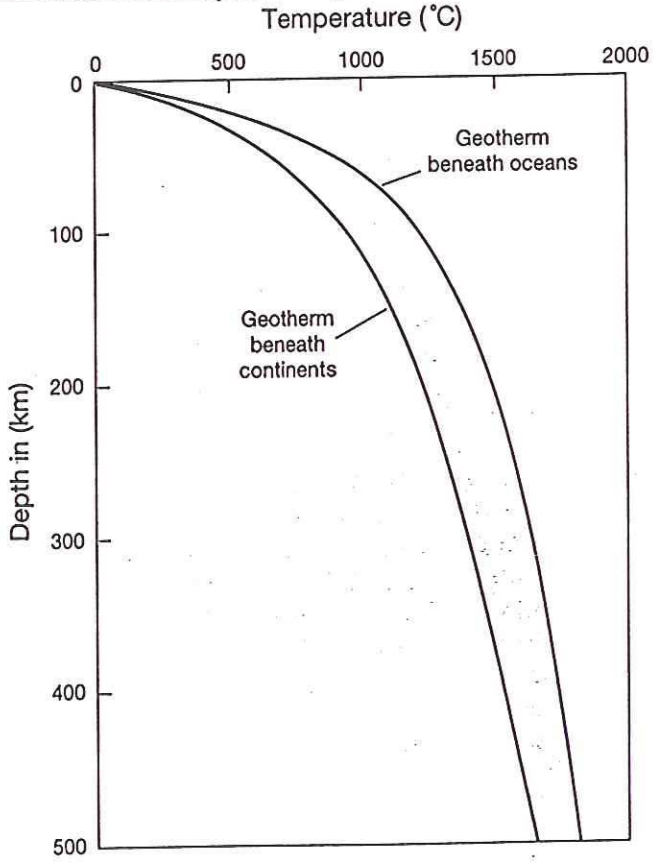

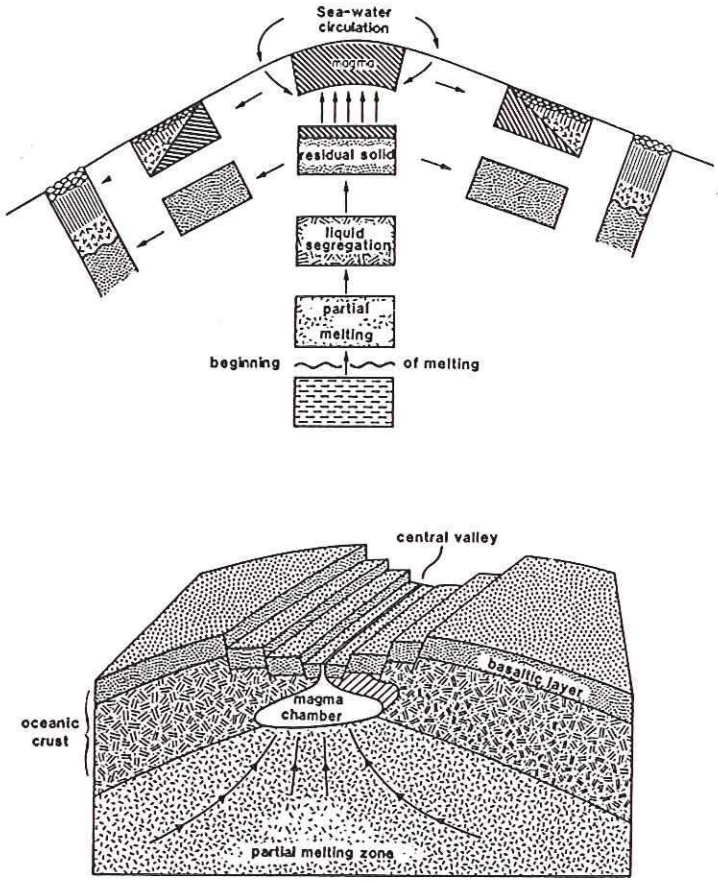


FIGURE 55 The creation of oceanic lithosphere. Material from the mantle rises beneath a ridge axis. During its ascent melting occurs and the liquid thus formed rises faster than surrounding unmelted material. Near the surface the liquid (which forms the crust) cools and interacts with seawater. Then the liquid and residual material spread horizontally away from the spreading axis. On the bottom is a block diagram of a slow-spreading ridge (spreading at, say, a rate on the order of 2 centimeters per year) that shows how the processes of lithosphere creation may occur in a more realistic scenario.

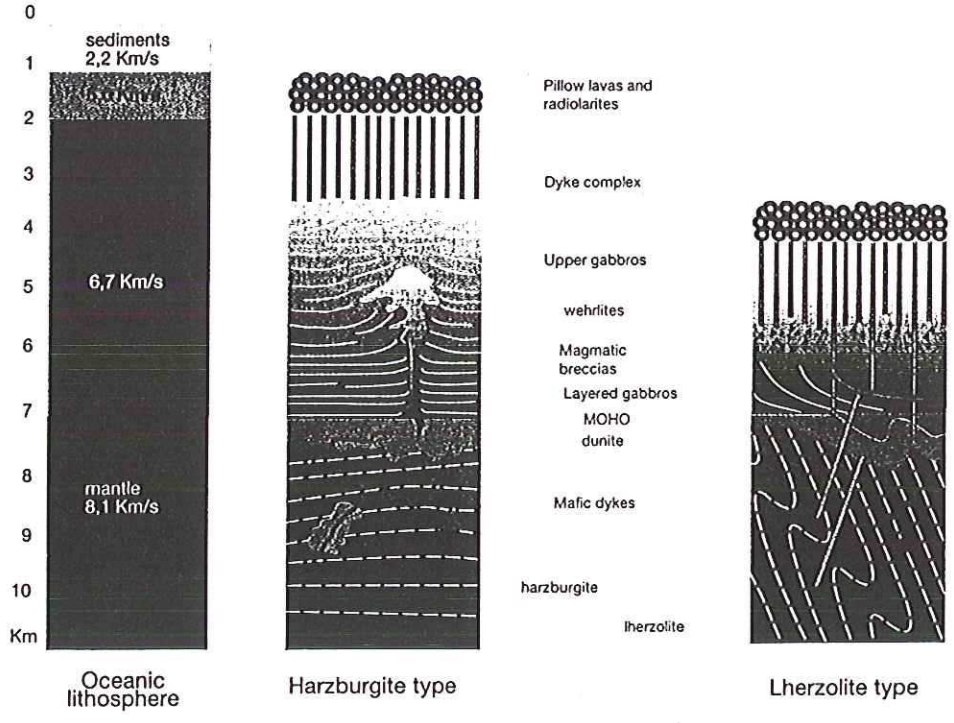


**Figure 5.8**
Columns comparing the structure of the oceanic crust as defined seismically with the two main types of ophiolites: the harzburgite type as illustrated by the Oman ophiolites and the lherzolite type, by the Trinity ophiolites of California. (After F. Boudier and A. Nicolas 1985, Earth Planet. Sci. Lett., 76, 84–92)

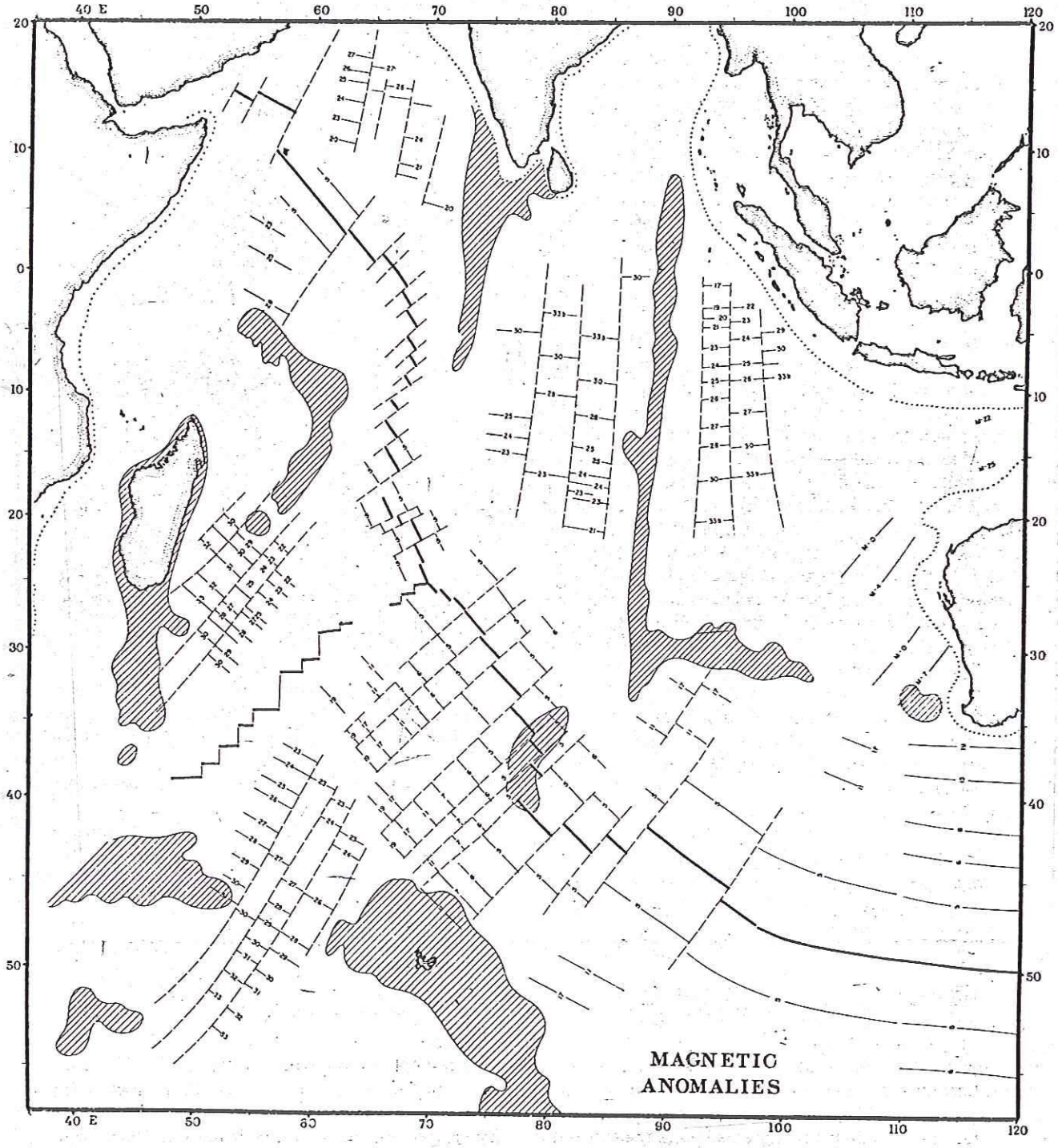


Fig. 6. Identifiable magnetic anomalies in Indian Ocean. For sources, see text. Hachures represent shoal regions of Figure 1.

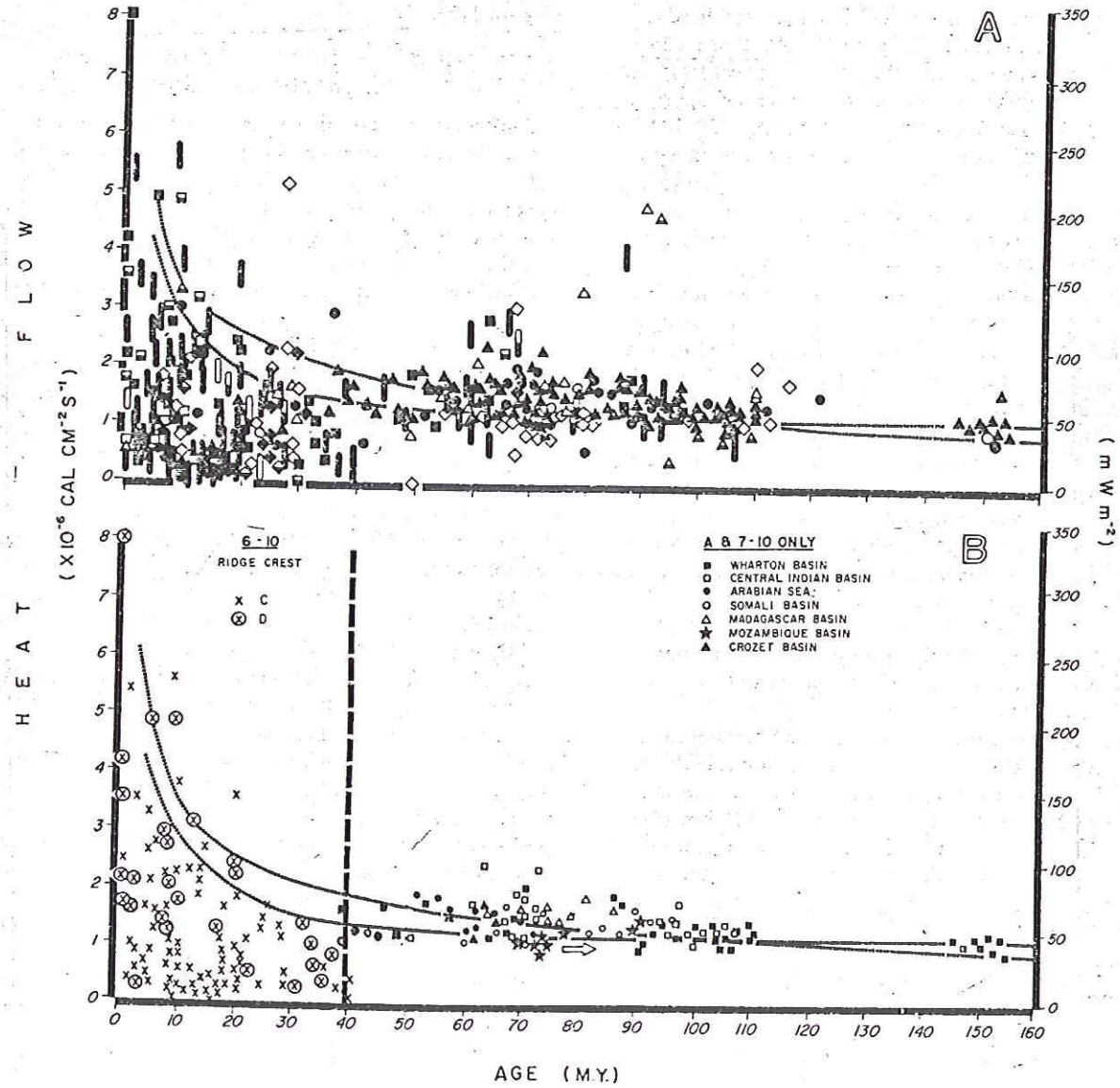


Fig. 9. Heat flow versus age in the Indian Ocean. (*a*) All the data. (*b*) Filtered data. Notice that the filtering removes much scatter but does not change the mean of values older than 50 m.y. B.P. The arrow refers to the Mozambique Basin values that appear to be from older sea floor than that indicated by DSDP hole ages in the basin. Solid curves are from *Sclater and Francheteau* [1970] and *Parker and Oldenburg* [1973].

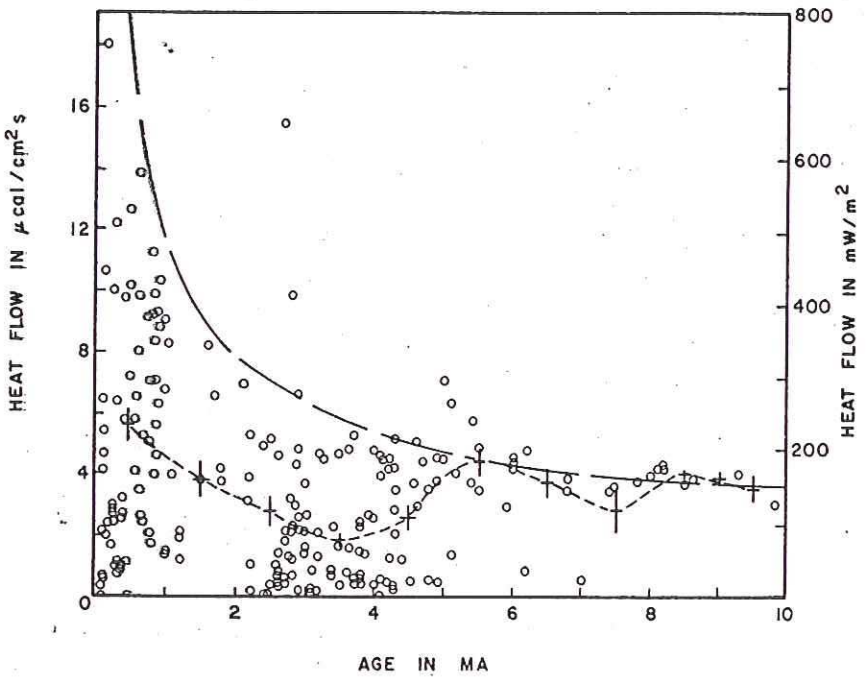


Fig. 5. Heat flow values plotted as a function of age on the Galapagos spreading center. Only those values which are on oceanic crust of well-defined age were used for this plot. Circles represent heat flow values. Pluses are 1-m.y. means. The long-dashed curve is the heat flow expected from the thermal model of *Parsons and Sclater* [1977], and the short-dashed curve connects the mean of the observed data [after *Anderson and Hobart,* 1976].